



Identification of Clotrimazole Derivatives as Specific Inhibitors of Arenavirus Fusion

Giulia Torriani,^a Evgeniya Trofimenko,^b Jennifer Mayor,^a Chiara Fedeli,^a Hector Moreno,^a Sébastien Michel,^b Mathieu Heulot,^b Nadja Chevalier,^b  Gert Zimmer,^{c,d} Neeta Shrestha,^e Philippe Plattet,^e Olivier Engler,^f Sylvia Rothenberger,^{a,f} Christian Widmann,^b Stefan Kunz^a

^aInstitute of Microbiology, Lausanne University Hospital, Lausanne, Switzerland

^bDepartment of Physiology, Faculty of Biology and Medicine, University of Lausanne, Lausanne, Switzerland

^cInstitute of Virology and Immunology, Mithras, Switzerland

^dDepartment of Infectious Diseases and Pathobiology, Vetsuisse Faculty, University of Bern, Bern, Switzerland

^eDivision of Neurological Sciences, Vetsuisse Faculty, University of Bern, Bern, Switzerland

^fSpiez Laboratory, Spiez, Switzerland

ABSTRACT Arenaviruses are a large family of emerging enveloped negative-strand RNA viruses that include several causative agents of viral hemorrhagic fevers. For cell entry, human-pathogenic arenaviruses use different cellular receptors and endocytic pathways that converge at the level of acidified late endosomes, where the viral envelope glycoprotein mediates membrane fusion. Inhibitors of arenavirus entry hold promise for therapeutic antiviral intervention and the identification of “drugable” targets is of high priority. Using a recombinant vesicular stomatitis virus pseudotype platform, we identified the clotrimazole-derivative TRAM-34, a highly selective antagonist of the calcium-activated potassium channel KCa3.1, as a specific entry inhibitor for arenaviruses. TRAM-34 specifically blocked entry of most arenaviruses, including hemorrhagic fever viruses, but not Lassa virus and other enveloped viruses. Anti-arenaviral activity was likewise observed with the parental compound clotrimazole and the derivative senicapoc, whereas structurally unrelated KCa3.1 inhibitors showed no antiviral effect. Deletion of KCa3.1 by CRISPR/Cas9 technology did not affect the antiarenaviral effect of TRAM-34, indicating that the observed antiviral effect of clotrimazoles was independent of the known pharmacological target. The drug affected neither virus-cell attachment, nor endocytosis, suggesting an effect on later entry steps. Employing a quantitative cell-cell fusion assay that bypasses endocytosis, we demonstrate that TRAM-34 specifically inhibits arenavirus-mediated membrane fusion. In sum, we uncover a novel antiarenaviral action of clotrimazoles that currently undergo *in vivo* evaluation in the context of other human diseases. Their favorable *in vivo* toxicity profiles and stability opens the possibility to repurpose clotrimazole derivatives for therapeutic intervention against human-pathogenic arenaviruses.

IMPORTANCE Emerging human-pathogenic arenaviruses are causative agents of severe hemorrhagic fevers with high mortality and represent serious public health problems. The current lack of a licensed vaccine and the limited treatment options makes the development of novel antiarenaviral therapeutics an urgent need. Using a recombinant pseudotype platform, we uncovered that clotrimazole drugs, in particular TRAM-34, specifically inhibit cell entry of a range of arenaviruses, including important emerging human pathogens, with the exception of Lassa virus. The antiviral effect was independent of the known pharmacological drug target and involved inhibition of the unusual membrane fusion mechanism of arenaviruses. TRAM-34 and its derivatives currently undergo evaluation against a number of human diseases and show favorable toxicity profiles and high stability *in vivo*. Our study provides the

Citation Torriani G, Trofimenko E, Mayor J, Fedeli C, Moreno H, Michel S, Heulot M, Chevalier N, Zimmer G, Shrestha N, Plattet P, Engler O, Rothenberger S, Widmann C, Kunz S. 2019. Identification of clotrimazole derivatives as specific inhibitors of arenavirus fusion. *J Virol* 93:e01744-18. <https://doi.org/10.1128/JVI.01744-18>.

Editor Terence S. Dermody, University of Pittsburgh School of Medicine

Copyright © 2019 American Society for Microbiology. All Rights Reserved.

Address correspondence to Christian Widmann, christian.widmann@unil.ch, or Stefan Kunz, stefan.kunz@chuv.ch.

S.R., C.W., and S.K. are co-senior authors.

Received 3 October 2018

Accepted 21 December 2018

Accepted manuscript posted online 9 January 2019

Published 5 March 2019

basis for further evaluation of clotrimazole derivatives as antiviral drug candidates. Their advanced stage of drug development will facilitate repurposing for therapeutic intervention against human-pathogenic arenaviruses.

KEYWORDS antiviral agents, arenavirus, emerging virus, fusion inhibitor, viral entry, viral fusion, viral hemorrhagic fever

Mammalian arenaviruses are a large family of emerging enveloped negative-strand viruses divided into two major groups, the Old World and the New World arenaviruses. The Old World group includes the prototypic lymphocytic choriomeningitis virus (LCMV) that is a relevant human pathogen in transplantation and pediatric medicine (1, 2). The highly pathogenic Lassa virus (LASV) causes a severe viral hemorrhagic fever with high mortality in Western Africa (3). Lujo virus (LUJV) emerged in 2008 in Southern Africa and was associated with a cluster of fatal human hemorrhagic fever cases (4). The New World arenaviruses are organized into four clades, A, B, C, and D (5). The highly pathogenic South American hemorrhagic fever viruses Junin (JUNV), Machupo (MACV), Guanarito (GTOV), Sabia virus (SABV), and Chapare virus (CHAV) belong to clade B and group with closely related nonpathogenic viruses, including Tacaribe (TCRV) and Amapari virus (AMPV). New World viruses of clade A and C have so far not been associated with human disease, whereas the disease potential of clade D viruses remains unclear (5). Human infection with pathogenic arenaviruses occurs mainly via reservoir-to-human transmission by inhalation of aerosolized rodent excreta, skin abrasions, or ingestion of contaminated food (5, 6). After initial multiplication at the site of entry, the virus disseminates systemically in severe infection, and serum viral load is predictive for disease outcome (7, 8). Due to their transmissibility via aerosol (9) and high lethality, hemorrhagic arenaviruses are considered category A select agents by the Centers for Disease Control (10). The current lack of a licensed vaccine and limited treatment options make the development of novel antiviral therapeutics an urgent need.

Arenaviruses are characterized by a nonlytic life cycle confined to the cytosol (11). Their genome is comprised of two RNA segments with ambisense coding strategy. A small (S) RNA of 3.4 kb encodes the envelope glycoprotein precursor (GPC) and the nucleoprotein (NP). The large (L) segment (7.2 kb) encodes the matrix protein (Z) and the viral RNA-dependent RNA polymerase L. The envelope GPC precursor undergoes processing, by signal peptidases and by the proprotein-convertase subtilisin kexin isozyme-1/site-1 protease (SKI-1/S1P) to yield an unusually stable signal peptide (SSP), an N-terminal GP1 moiety, and the membrane-anchored GP2 (12). The mature arenavirus envelope GP in its metastable prefusion conformation forms a trimer of SSP/GP1/GP2 heterotrimers (12–15). The GP1 subunit binds to cellular receptors and defines viral tropism (16, 17), whereas GP2 drives viral membrane fusion. The receptor for Old World and clade C New World arenaviruses is the extracellular matrix receptor dystroglycan (DG) (18, 19), whereas LUJV uses the semaphorin receptor neuropilin 2 (NRP2) (20). The clade B New World arenaviruses use cargo receptor transferrin receptor 1 (TfR1). Human-pathogenic arenaviruses recognize the human TfR1 form, linking receptor specificity to human disease potential (21–23). In addition, cell surface receptors of the T-cell immunoglobulin and mucin receptor (TIM) and Tyro3/Axl/Mer (TAM) families, as well as C-type lectins such as DC-SIGN, can contribute to arenavirus entry, in particular in the absence of the main receptors (24–27). After receptor-mediated endocytosis, arenaviruses are delivered to late endosomes (28), where a low pH triggers fusion (29). The transmembrane GP2 undergoes low-pH-induced conformational changes, including the transition of the metastable prefusion state, to an energetically favorable postfusion state with a six-helix bundle architecture reminiscent of other class I viral fusion proteins (30, 31). The triggering of LASV and LUJV fusion critically depends on the late endosomal proteins lysosome-associated membrane protein 1 (LAMP-1) and CD63, respectively, which act as intracellular entry factors (20, 32).

Considering the correlation between viral load early in infection and disease out-

come in human arenavirus hemorrhagic fevers (7, 8), drugs targeting viral entry may limit viral dissemination, providing the patient's immune system a window to develop an antiviral immune response to control infection. A challenge for the development of direct antiviral agents against arenaviruses is the still limited structural information available. However, as arenaviruses critically depend on the cellular machinery for host cell invasion, the identification of "druggable" cellular factors required for productive viral infection appears as promising complementary strategy. This is illustrated by the identification of voltage-gated calcium channels (VGCC) as novel arenavirus entry factors in a recent RNAi silencing screen (33). The development of antiarenaviral drugs "from scratch" is a daunting task, in particular considering the limited resources at hand. Clinically approved drugs or advanced drug candidates against other human diseases may be repurposed for antiviral intervention. This is highlighted by the therapeutic efficacy of clinically approved VGCC inhibitors against JUNV (33), providing proof-of-concept.

Ion channels represent a major class of drug targets implicated in a plethora of human disorders. Inspired by the identification of VGCC as novel targets for antiarenaviral intervention (33), we sought to identify other ion channels as possible candidates for arenavirus entry. Our search criteria included tissue-specific expression pattern matching arenaviral tropism, implication in infection with other intracellular pathogens, and availability of specific inhibitors at advanced stages of drug development. The intermediate conductance calcium-activated potassium channel KCa3.1, encoded by the gene KCNN4, consists of six transmembrane domains that form heterotetramers, which regulate efflux of potassium ions. In humans, KCa3.1 channels are expressed in major cell types infected by arenaviruses during early infection, including epithelial cells, endothelial cells, and different immune cells (34–38). KCa3.1 has been evaluated as a drug target for important human diseases, including sickle cell anemia (39), vascular disease (40), obliterative airway disease (41), and malaria, which is caused by infection with the intracellular parasite *Plasmodium* (42). Considering the therapeutic promise of KCa3.1 channels, several peptide-based and small molecule inhibitors have been developed (34). The best characterized among them are clotrimazole {1-[(2-chlorophenyl) diphenylmethyl]-1H-imidazole} and its derivatives TRAM-34 [1-[(2-chlorophenyl) diphenylmethyl]-1H-pyrazole] (43), and ICA-17043 [senicapoc; 2,2-bis(4-fluorophenyl)-2-phenylacetamide] (44). TRAM-34 and senicapoc block KCa3.1 with a 50% inhibitory concentration (IC_{50}) of 11 to 25 nM and show >200-fold selectivity over other potassium, calcium, sodium, and chloride channels (34). The low IC_{50} , favorable toxicity profile, and exquisite specificity (34, 39, 45) made TRAM-34 a powerful molecular probe to uncover a possible role of KCa3.1 channels in viral entry. Using a recombinant vesicular stomatitis virus (VSV) pseudotype platform, we screened TRAM-34 against a range of emerging enveloped viruses and found that the drug specifically inhibits cell entry of arenaviruses. The antiviral effect was independent of its pharmacological target KCa3.1 but critically depended on the triarylmethane backbone of the drug. TRAM-34 neither affected virus-receptor binding nor endocytosis but specifically blocked arenavirus fusion. In sum, we reveal a novel and unexpected antiarenaviral action of clotrimazoles, opening the possibility to repurpose these drugs for therapeutic intervention.

RESULTS

The clotrimazole-derivative TRAM-34 inhibits infection with pseudotype viruses containing the envelope glycoproteins of various arenaviruses. A major challenge for the evaluation of candidate drug compounds against highly pathogenic emerging viruses are the strict biosafety requirements that limit work with these pathogens to BSL4 facilities. By the process of pseudotyping, viral glycoproteins provided in *trans* can be incorporated into recombinant vesicular stomatitis virus in which the glycoprotein gene (G) was deleted (rVSVΔG) and replaced with reporter genes, such as enhanced green fluorescent protein (EGFP) and luciferase (Luc) (46). The resulting "VSV pseudotypes" are replication competent but unable to propagate,

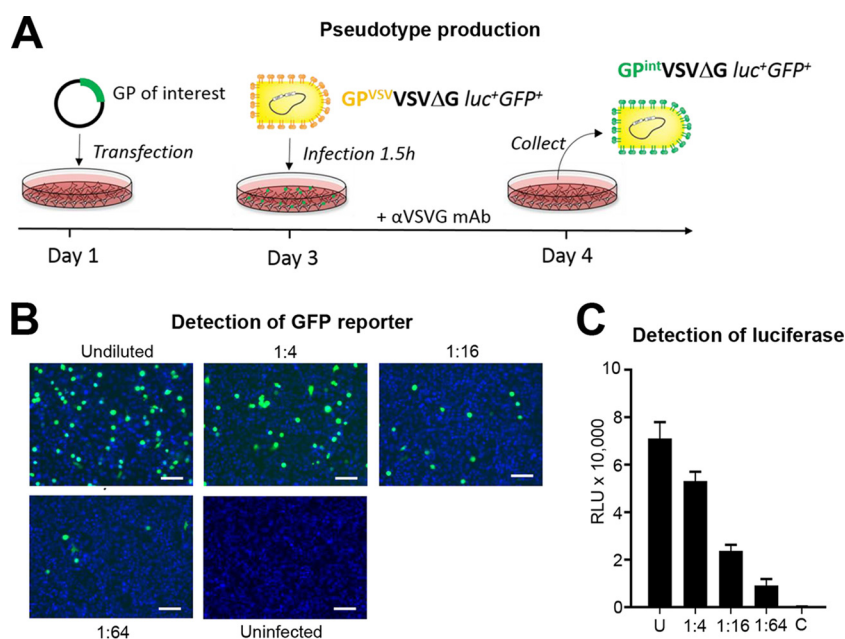


FIG 1 Recombinant VSV vectors pseudotyped with GPs of emerging viruses. (A) Pseudotype production. HEK 293F cells were transfected with an expression plasmid encoding the recombinant viral GP of interest. Transfected cells were infected with replication-competent recombinant VSVΔG⁺GFP⁺ pseudotypes that contains a luciferase and EGFP reporter and lack the ORF for endogenous VSV G. Efficient entry was mediated by recombinant VSV G (GP^{VSV}) in the envelope of the pseudotypes. Virus production in the presence of a neutralizing MAb to VSV G (αVSVG MAb) efficiently neutralized residual GP^{VSV}VSVΔG⁺GFP⁺ and specifically yielded VSVΔG⁺GFP⁺ pseudotypes decorated with the heterologous GP of interest (GP^{int}) provided in *trans*. (B) Pseudotype infection. Monolayers of A549 cells were infected with serial dilutions of VSVΔG⁺GFP⁺ pseudotypes bearing VSV G, followed by detection of the EGFP reporter by direct fluorescence microscopy after 24 h. Nuclei stained with NucBlue appear in blue. Scale bar, 100 μm. (C) Quantification of pseudotype infection with luciferase. Cells infected as in panel B were subjected to luciferase assay after 24 h as detailed in Materials and Methods. The data are means of relative luminescence units (RLU) + the standard deviations (SD; *n* = 3). Please note the correlation between GFP-positive cells in panel B and the luciferase signal in panel C.

making them suitable for work under BSL2 conditions (Fig. 1A). Since virus cell attachment and entry are mediated exclusively by the viral envelope proteins, these VSV pseudotypes represent powerful BSL2 surrogates to evaluate candidate viral entry drugs (47). For our purposes, we generated recombinant VSV pseudoparticles bearing the GPs of the Old World arenavirus LCMV (isolate ARM53b clone-13), LASV, LUJV, the South American clade B hemorrhagic fever viruses MACV and GTOV, the nonpathogenic clade B New World arenaviruses AMPV and TCRV, and the clade D New World virus Tamiami (TAMV). We further generated VSV pseudotypes bearing the GPs of the filovirus Ebola (EBOV), the Orthohantaviruses Hantaan (HTNV) and Andes (ANDV), as well as VSV. Depending on the heterologous viral GP provided in *trans*, pseudotyping may occur rather inefficiently, resulting in unfavorable signal/background ratios due to the presence of residual VSV G in the production system (Fig. 1A). To optimize the experimental window of our system, rVSV pseudotypes were produced in the presence of the potent neutralizing anti-VSV G MAb I-1 (48), resulting in virtually negligible background. Using this approach, rVSV pseudoparticles were produced with high efficiency, yielding robust specific titers (10^5 to 10^8 PFU/ml). Serial dilutions of pseudotypes were added to fresh monolayers of human lung epithelial A549 cells and infection assessed by direct fluorescence microscopy scoring EGFP-expressing cells (Fig. 1B). Measurement of luciferase activity in parallel specimens revealed a robust correlation between the number of EGFP-expressing cells and luminescence levels (Fig. 1C), allowing the use of the luciferase reporter to quantify infection in a semi-high-throughput assay format.

Since many emerging human-pathogenic viruses are transmitted via aerosols (10), we used A549 human lung epithelial cells that express KCa3.1 channels as a suitable

model. To minimize the duration of drug exposure and unwanted off-target effects, we performed a previously established drug washout assay (49) (Fig. 2A). Briefly, confluent monolayers of A549 cells were pretreated for 30 min with the drug, followed by infection with VSV pseudotypes at low multiplicity (multiplicity of infection [MOI] = 0.05) in the presence of drug. After 90 min, the drug was washed out using medium supplemented with 20 mM the lysosomotropic agent ammonium chloride. When added to cells, ammonium chloride raises the endosomal pH instantly and blocks low pH-dependent endosomal escape of viruses, without causing overall cytotoxicity (50, 51). To exclude possible toxicity of TRAM-34, we measured intracellular ATP levels of cells treated with increasing drug concentrations using CellTiter-Glo assay and observed no significant effect on A549 cell viability with up to 100 μ M TRAM-34 (Fig. 2B), in line with published data (34). TRAM-34 blocked infection with most arenavirus VSV pseudotypes at low micromolar concentration in a dose-dependent manner, including MACV, GTOV, AMPV, TCRV, LCMV, LUJV, and TAMV (Fig. 2C). In contrast, LASV pseudotypes seemed relatively resistant against the drug (Fig. 2C). At concentrations up to 20 μ M, TRAM-34 showed no activity against pseudotypes of HTNV, ANDV, EBOV, and VSV, indicating specificity against arenaviruses (Fig. 2C). We validated the inhibition of selected arenavirus pseudotypes with TRAM-34 in human cervix epithelial (HeLa) cells and observed comparable specific inhibition (Fig. 2D).

The TRAM-34-sensitive arenaviruses included pathogenic clade B viruses (Fig. 2C) that use human TfR1 and clathrin-mediated endocytosis for cell entry (21, 52, 53). We therefore tested whether TRAM-34 affected the endogenous function of TfR1 as a cargo receptor, monitoring internalization of fluorescent-labeled human transferrin in HeLa cells in presence and absence of drug using flow cytometry (Fig. 2E). In contrast to the robust inhibition of clade B arenavirus pseudotype infection (Fig. 2C), TRAM-34 had no significant effect on transferrin uptake via clathrin-mediated endocytosis, suggesting a specific antiviral effect of the drug without general perturbation of endocytosis (Fig. 2E).

TRAM-34 inhibits arenavirus entry, but not later infection steps. To validate the antiviral effect of TRAM-34 against authentic virus, we chose live TCRV as well-established BSL2 model for New World arenaviruses. TCRV belongs to the clade B New World arenaviruses, where it groups in the same sublineage together with the highly pathogenic JUNV and MACV. Despite this close phylogenetic relationship, TCRV causes only mild self-limiting febrile illness in humans and can be handled at BSL2 (5). Briefly, A549 cells were pretreated for 30 min with the inhibitor, followed by infection with TCRV at low multiplicity (MOI = 0.01) in the presence of drug (Fig. 3A). After 1 h, the drug was washed out using medium supplemented with 20 mM ammonium chloride to prevent secondary infection. After 16 h, cells were fixed and productive infection quantified by detection of TCRV NP by immunofluorescence assay (IFA) using a specific monoclonal antibody (MAB). Consistent with the pseudotype data, TRAM-34 reduced infection of live TCRV in a dose-dependent manner (Fig. 3B). To validate cell entry as the main target of TRAM-34, we performed “time-of-addition” experiments with live virus (Fig. 3B). Consistent with the pseudotype data, the inhibitor was only active against TCRV when added before or during infection, but it had little effect at later time points postentry (Fig. 3B), confirming that TRAM-34 specifically inhibits arenavirus entry but not later steps of the viral infection cycle. To assess possible effects of TRAM-34 on virus propagation and infectious virus production, monolayers of A549 cells were pretreated with TRAM-34, followed by infection with TCRV, recombinant LCMV, and a recombinant LCMV expressing LASV GP (rLCMV-LASVGP), whose cellular tropism closely resembles authentic LASV (24, 54, 55) at low multiplicity. For comparison, we included 5-(*N*-ethyl-*N*-isopropyl)-amiloride (EIPA) that blocks sodium proton exchangers (56, 57) and is a potent inhibitor of cell entry of the Old World arenaviruses LCMV and LASV (58). In addition, we included the specific SKI-1/S1P inhibitor PF429242 that blocks arenavirus GPC processing and prevents production of infectious virus from infected cells (59, 60). As shown in Fig. 3C, TRAM-34 reduced infectious virus production for TCRV and LCMV,

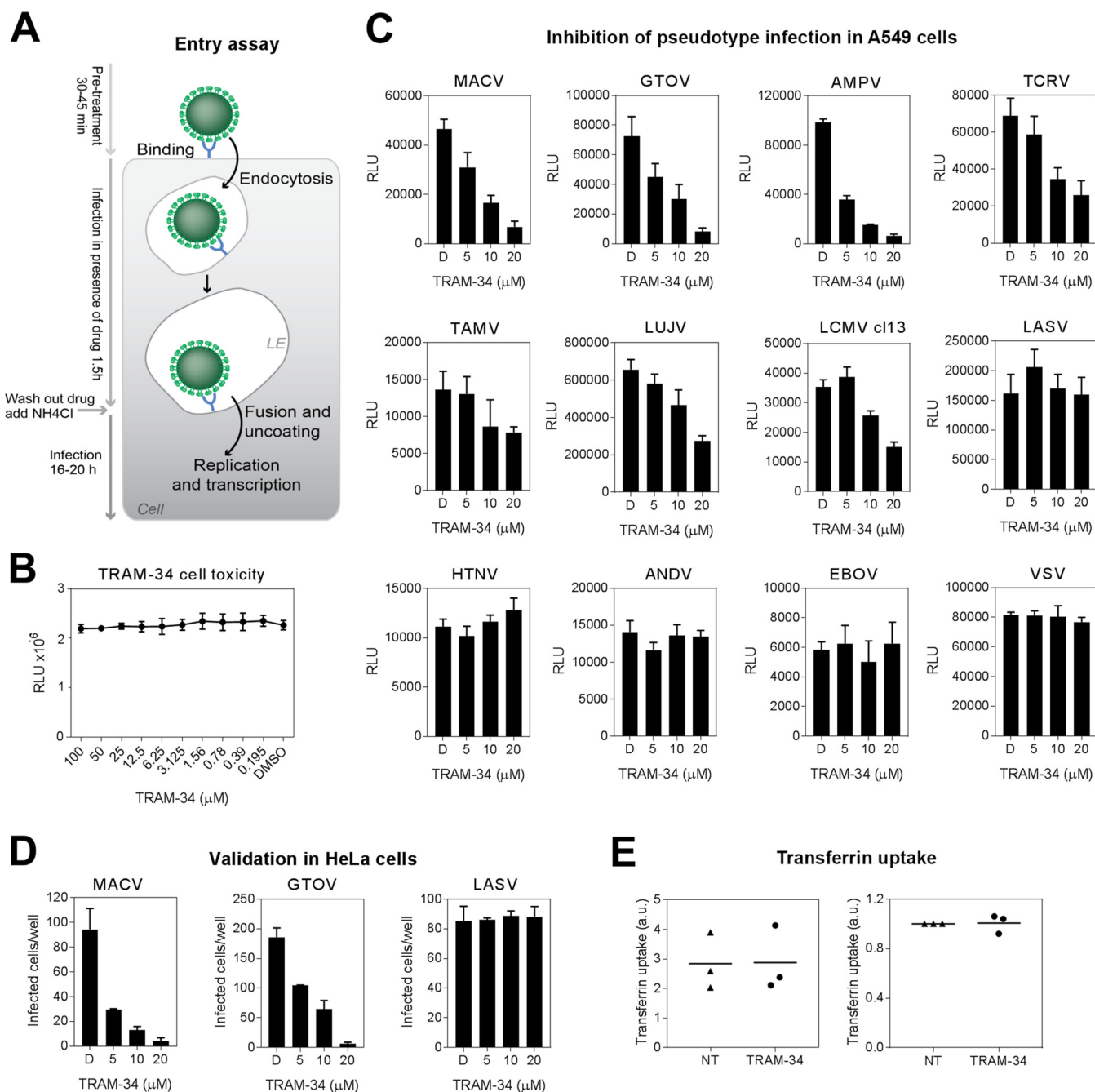


FIG 2 The clotrimazole derivative TRAM-34 inhibits arenavirus pseudotype infection. (A) Schema of the entry assay. For details, please see the text. LE, late endosome. (B) TRAM-34 shows no overt toxicity up to 100 μ M. Monolayers of A549 cells were treated with the indicated concentrations of TRAM-34 under the assay condition (A). After 24 h, intracellular ATP levels were detected using a CellTiter-Glo assay as detailed in Materials and Methods. The data are means of RLU + the SD ($n = 3$). Please note the negligible reduction in cellular ATP levels after exposure to up to 100 μ M drug. (C) Infection of several arenavirus VSV pseudotypes is specifically inhibited by TRAM-34. Monolayers of A549 cells were pretreated with increasing concentrations of TRAM-34 or DMSO vehicle alone (D) for 30 min, followed by infection with the indicated VSV pseudotype viruses at an MOI of 0.05 in the presence of drug. After 1.5 h, cells were washed three times with medium supplemented with 20 mM ammonium chloride, followed by 16 h of incubation in the presence of the lysosomotropic agent. Infection was detected by luciferase assay as in (Fig. 1C). The data are means of RLU + the SD ($n = 3$). (D) Validation of selected pseudotypes in HeLa cells. Monolayers of HeLa cells were pretreated with increasing concentrations of TRAM-34, followed by infection with the indicated VSV pseudotype viruses at an MOI of 0.01 in the presence of drug. Infection was determined by counting EGFP⁺ infected cells. The data are means + the SD ($n = 3$). (E) TRAM-34 does not interfere with the endogenous function of TfR1. Monolayers of HeLa cells were pretreated or not (NT) with 20 μ M TRAM-34 for 30 min. Cells were then incubated in the presence of 20 μ g/ml Alexa 488-conjugated transferrin for 20 min. To quantify transferrin uptake, cells were detached by trypsin and single cells suspensions subjected to trypan blue treatment in order to quench the cell surface fluorescence. Intracellular transferrin was quantified by flow cytometry. The data are the mean fluorescence intensities of three biological replicates, with the means indicated.

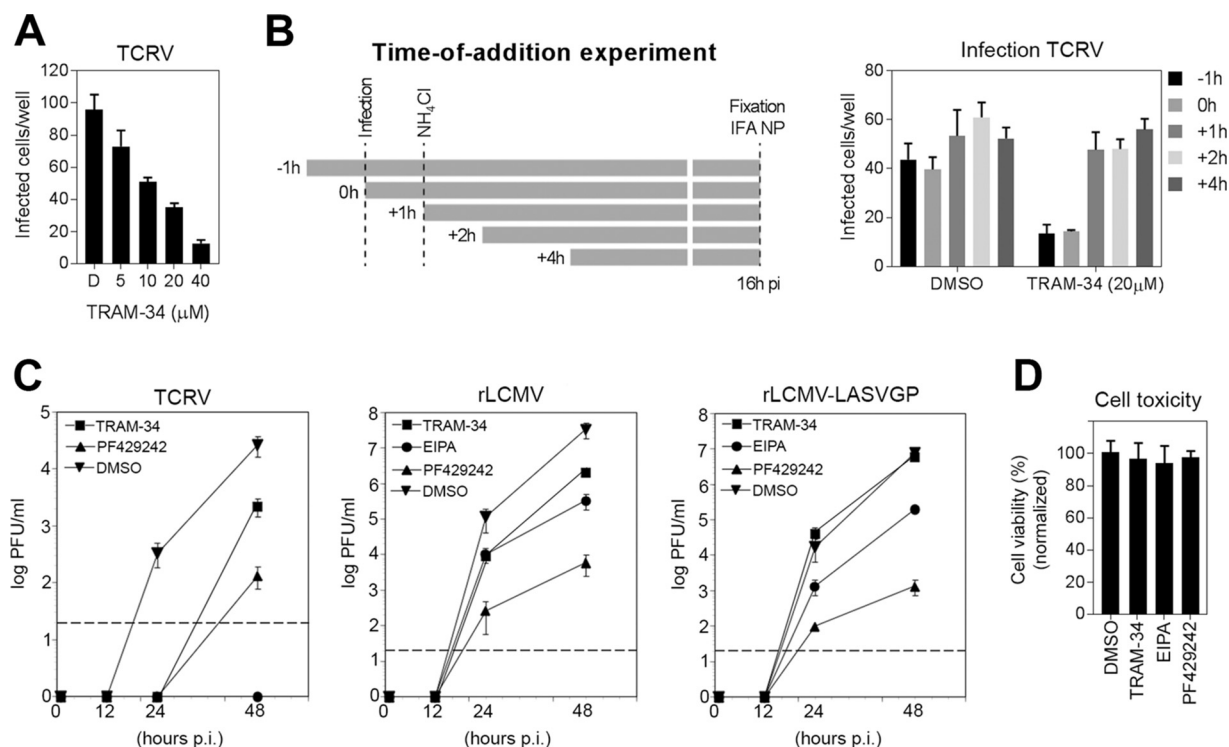


FIG 3 TRAM-34 inhibits arenavirus entry. (A) TRAM-34 inhibits infection with live TCRV. A549 cells were pretreated with TRAM-34 at increasing concentrations for 30 min, followed by infection with TCRV at 200 PFU/well in the presence of drug. After 1 h, cells were washed three times with medium containing 20 mM ammonium chloride, followed by 16 h of incubation in the presence of the lysosomotropic agent. After 16 h of incubation in the presence of ammonium chloride, cells were fixed and infection detected by IFA using a specific MAb to TCRV NP, combined with a Alexa 488-conjugated secondary antibody. Infection was quantified by counting infected cells per well considering cell doublets as single infection events. The data are means \pm the SD ($n = 3$). (B) Time-of-addition experiment. A549 cells were infected with TCRV (200 PFU/well), and TRAM-34 was added at different time points pre- or postinfection at 20 μ M. Virus was added at time point 0, followed by washing and the addition of ammonium chloride after 1 h. Ammonium chloride was kept throughout the experiment, and the cells were subjected to IFA after 16 h as described in panel A. (C) Monolayers of A549 cells were pretreated with TRAM-34 (40 μ M), EIPA (20 μ M), PF429242 (20 μ M), or DMSO control for 30 min, followed by infection with TCRV, rLCMV, and rLCMV-LASVGP at low multiplicity (MOI = 0.01). At the indicated time points, the virus titers in the conditioned cell culture supernatant were determined by an immunofocus assay with a detection limit of 20 PFU/ml (dashed lines). The data are means \pm the SD ($n = 3$). (D) Cell toxicity of drugs was assessed after 48 h by the CellTiter-Glo assay. The data are means \pm the SD ($n = 3$).

but not rLCMV-LASVGP, in line with the pseudotype data (Fig. 2C and D). As expected, the entry inhibitors TRAM-34 and EIPA were less potent inhibitors of infectious virus production than the SKI-1/S1P inhibitor that blocks a late step in viral infection and efficiently prevents release of infectious virus progeny from infected cells (58–60). None of the drugs showed significant toxicity at the concentrations used (Fig. 3D).

Resistance of LASV GP against TRAM-34 is independent of LAMP-1. All arenavirus GP pseudotypes tested so far were sensitive to TRAM-34, with the notable exception of LASV pseudotypes (Fig. 2C and D). This was rather unexpected since the GPs of LASV and LCMV are structurally and functionally closely related (13, 14). To exclude an artifact of our VSV-based pseudotype system, we validated the dose-response characteristic for TRAM-34 against LCMV and rLCMV-LASVGP. As observed with the pseudotypes, TRAM-34 specifically inhibited infection with LCMV, but not rLCMV-LASVGP (Fig. 4A), mapping drug resistance to LASV GP.

The data at hand suggested that a particular feature of LASV GP-mediated cell entry not shared with other arenaviruses may confer resistance. Both LASV and LCMV attach to A549 cells via the high-affinity receptor DG, followed by internalization via macropinocytosis (58). However, in contrast to LCMV, cell entry of LASV critically depends on the endosomal resident protein LAMP-1 as a late endosomal entry factor (32). Following delivery to late endosomes, low pH destabilizes the high-affinity interaction between LASV GP1 and DG, resulting in a “receptor switch” and GP1 engagement of LAMP-1, which triggers membrane fusion. Structural and functional studies revealed a stable

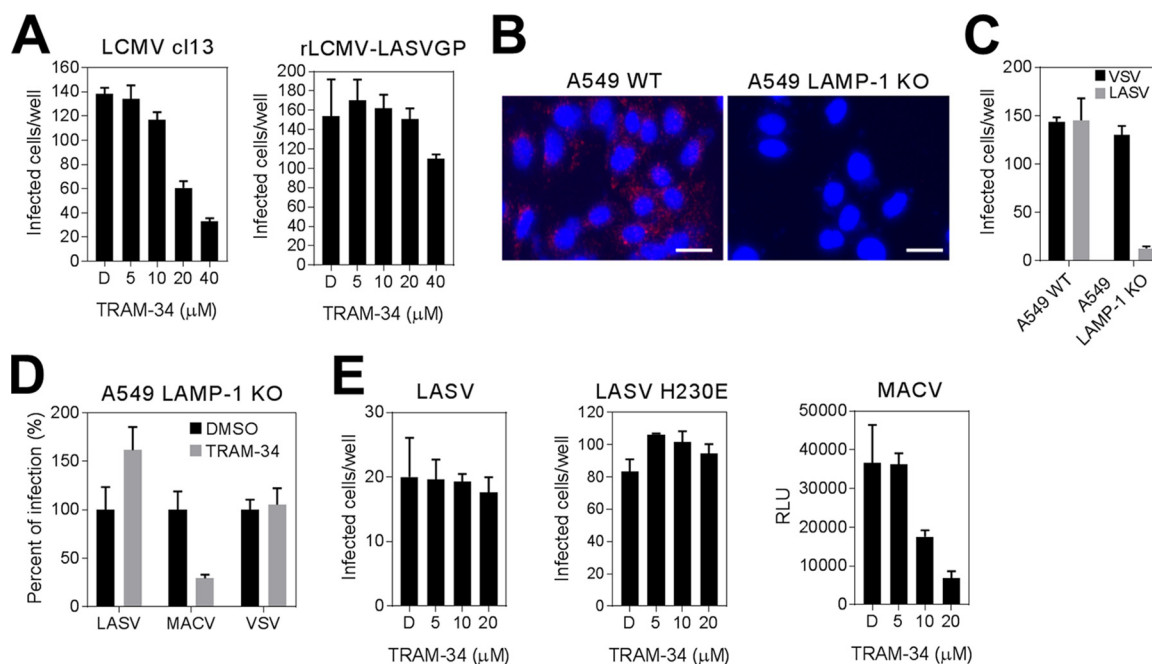


FIG 4 Resistance of LASV GP against TRAM-34 is independent of LAMP-1. (A) Specific inhibition of rLCMV-LASVGP infection by TRAM-34. A549 cells were pretreated with TRAM-34 at increasing concentrations for 30 min, followed by infection with rLCMV-LASVGP and LCMV clone-13 at 200 PFU/well in the presence of drug. After 1.5 h, the cells were washed, and medium containing 20 mM ammonium chloride was added. After 16 h, cells were fixed and infection detected by IFA using a specific MAb to LCMV NP, combined with an Alexa 488-conjugated secondary antibody. Infection was quantified as in Fig. 3B, and data are means + the SD ($n = 3$). (B) Generation of LAMP-1 null A549 cells. LAMP-1 was deleted from A549 cells by CRISPR/Cas9 technology as detailed in Materials and Methods, and depletion was verified by IFA with an anti-LAMP-1 antibody, combined with a rhodamine red-conjugated secondary antibody. Nuclei stained with DAPI appear in blue. Scale bar, 20 μm. (C) rVSVΔG-LASVGP infection of A549 cells depends on LAMP-1. (D) LAMP-1 null and control A549 cells were infected with rVSVΔG-LASVGP and rVSVΔG-VSVG at 200 PFU/well for 1 h. Infection was detected by direct fluorescence detection of the EGFP reporter as in Fig. 1B. The data are means + the SD ($n = 3$). (E) LAMP-1-independent LASV GP mutant H230E is TRAM-34 resistant. A549 cells were pretreated with TRAM-34 (20 μM) or solvent control (DMSO), followed by infection with the indicated VSV pseudotypes and infection assessed as in panel D. The data are means + the SD ($n = 3$).

“low pH conformation” of LASV GP1 containing a triad of histidine residues, which orchestrates fusion activity of LASV GP with the timing and location of the receptor switch (61–63). Membrane fusion triggering by LAMP-1 allows LASV to exit from earlier, less acidic endosomal compartments, avoiding prolonged exposure to the hostile environment (64). The capacity to use LAMP-1 as an endosomal entry factor is unique for LASV (65). We therefore hypothesized that resistance of LASV GP-mediated entry to TRAM-34 may be linked to LASV’s capacity to use LAMP-1 for fusion triggering. To test this possibility, we assessed the effect of TRAM-34 on LAMP-1-independent LASV entry. To this end, we depleted LAMP-1 from A549 cells using CRISPR/Cas9 technology, as detailed in Materials and Methods, and validated the LAMP-1 null phenotype by IFA (Fig. 4B). As expected, LAMP-1 null A549 cells showed markedly reduced susceptibility to LASV pseudotypes but still allowed significant LAMP-1-independent entry (Fig. 4C), as reported previously (64). The amount of virus infection observed in LAMP-1 null cells was sufficiently high to address a possible effect of TRAM-34 on LAMP-1-independent LASV entry. Similar to the situation in wild-type cells (Fig. 2A), TRAM-34 did not affect LAMP-1-independent infection of LASV pseudotypes (Fig. 4D). In a complementary approach, we used the LASV GP mutant H230E that bears a negative charge within the histidine triad, resulting in LAMP-1-independent fusion at higher pH (63). Like the wild type, pseudotypes bearing LASV GP H230E showed resistance to TRAM-34 (Fig. 4E). This indicates that the specific resistance of LASV GP to TRAM-34 was independent of LAMP-1-facilitated triggering of membrane fusion.

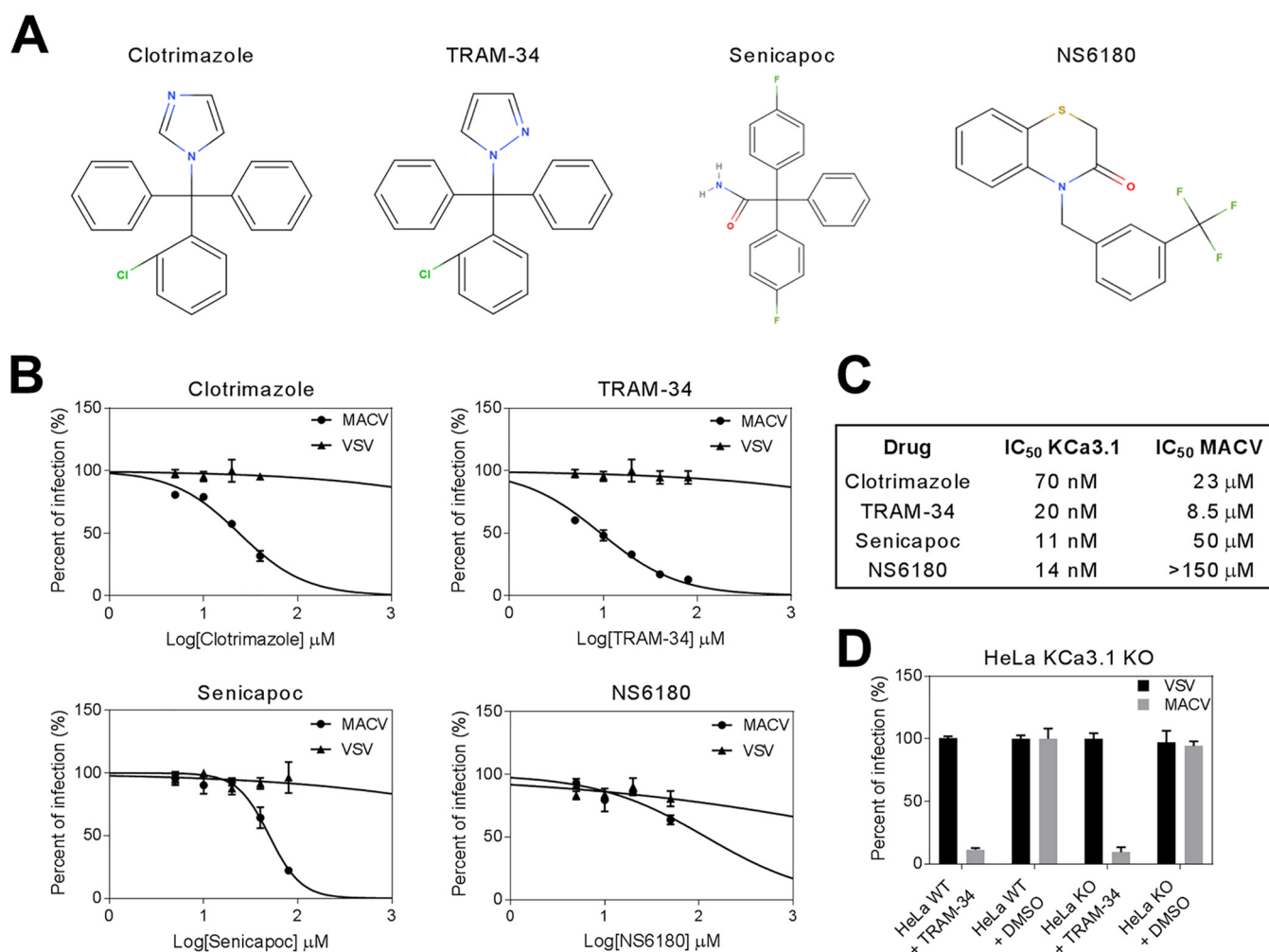


FIG 5 The antiviral effect of TRAM-34 is independent of its cellular target KCa3.1. (A) Structures of TRAM-34, clotrimazole, senicapoc, and NS6180. (B) Dose-response characteristics of candidate drugs against VSV pseudotypes displaying MACV GP or VSV G. Monolayers of A549 cells were pretreated with increasing drug concentrations for 30 min, followed by infection with the indicated pseudotypes and detection of infection as in Fig. 2B. (C) Apparent IC₅₀ of the tested drugs against MACV pseudotypes calculated from panel B compared to the reported IC₅₀ against the pharmacological drug target KCa3.1. Please note that the antiviral activity of drugs does not correlate with their published target-specific efficacy. (D) Deletion of KCa3.1 does not affect infection with MACV pseudotypes. Wild-type (WT) and KCa3.1 null HeLa cells were pretreated with TRAM-34 (20 μM) or solvent control (DMSO) and infected with the indicated VSV pseudotypes as in Fig. 2B. Infection was detected by direct fluorescence detection of the EGFP and the control (DMSO) set at 100%. The data are means \pm the SD ($n = 3$).

The antiviral effect of TRAM-34 is independent of its cellular target KCa3.1.

Next, we investigated if the observed specific inhibition of arenavirus cell entry was due to a direct effect of TRAM-34 on its pharmacological target KCa3.1. In a first approach, we compared the dose-response curves of TRAM-34 against susceptible MACV pseudotypes to the parental compound clotrimazole and the optimized TRAM-34-derivative senicapoc (Fig. 5A). TRAM-34 has an IC₅₀ for KCa3.1 of 20 nM, whereas senicapoc inhibits the channel with IC₅₀ of 11 nM (34). In addition, we included the structurally unrelated specific KCa3.1 inhibitor NS6180 with an IC₅₀ of 14 nM (66) (Fig. 5A). To exclude unspecific off-target effects of the drugs, we included VSV G pseudotypes, whose entry was not affected by any of the drugs tested, as a control. Both clotrimazole and senicapoc showed antiviral activity, albeit weaker than TRAM-34. In contrast, the KCa3.1 inhibitor NS6180 showed only weak activity against MACV pseudotypes with an IC₅₀ of >150 μM (Fig. 5B). Comparing the apparent IC₅₀ of the inhibitors against the virus and KCa3.1, we noted an apparent discrepancy between the reported on-target drug effects and antiviral activities (Fig. 5C). This gave a first hint that the observed antiviral effect may not be related directly to the known

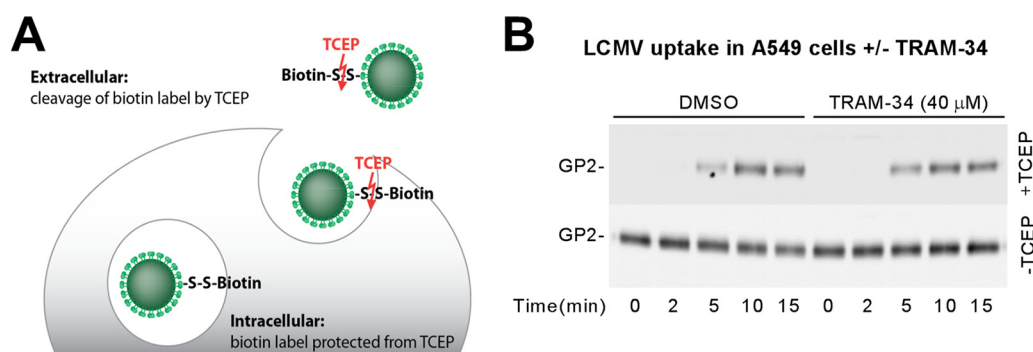


FIG 6 TRAM-34 affects neither virus-cell attachment nor endocytosis. (A) Schematic of the virus internalization assay (for details, please see text). (B) TRAM-34 does not affect virus-cell attachment and viral uptake. A549 cells were chilled on ice and incubated with biotin-S-S-labeled LCMV clone-13 (50 particles/cell) for 1 h in the cold. Unbound virus was removed and cells shifted to 37°C. After the indicated time points, cells were chilled on ice and treated with TCEP (+TCEP) or reaction buffer only (-TCEP). After quenching of residual TCEP, the cells were lysed, and the viral GP was isolated by IP with MAb 83.6 to LCMV GP2. Biotinylated GP2 was detected with streptavidin-HRP by Western blotting under nonreducing conditions using enhanced chemiluminescence (ECL). The upper blot (+TCEP) was exposed for 5 min; the lower blot (-TCEP) was exposed for 30 s.

pharmacological drug action. In a complementary approach, we therefore deleted the KCa3.1 channel from susceptible HeLa cells using CRISPR/Cas9 technology as described in Materials and Methods. Deletion of the channel showed only mild effects on cell viability and division rates. When infected with arenavirus pseudotypes, KCa3.1 null cells showed similar susceptibility than the wild type (Fig. 5D), suggesting a novel yet unknown anti-arenaviral effect by clotrimazoles. Moreover, the inhibitory effect of TRAM-34 occurred in KCa3.1 null and wild-type control cells to a similar extent (Fig. 5D).

TRAM-34 inhibits arenavirus GP fusion. Arenavirus entry is a complex, multistep process. We therefore tried to discern effects of TRAM-34 on virus attachment and endocytosis from later steps of viral entry. For this purpose, we used a well-established virus uptake assay developed originally by the Helenius laboratory that allows tracking of early steps of virus attachment and internalization (67–69). In this assay format, purified LCMV was labeled with the thiol-cleavable reagent NHS-SS-biotin, resulting in a biotin label sensitive to reducing agents that does not affect infectivity (Fig. 6A). Treatment with the membrane-impermeable reducing agent Tris(2-carboxyethyl)phosphine (TCEP) in the cold specifically cleaves the biotin label from virus exposed to the extracellular space, whereas the biotin label on internalized virus particles becomes resistant and can be detected using streptavidin (Fig. 6A). Monolayers of A549 cells were pretreated with TRAM-34 for 30 min at 37°C, chilled on ice, and incubated with biotin-labeled LCMV clone-13 (50 particles/cell) in the presence of drug for 1 h in the cold. Unbound virus was removed, and cells were rapidly shifted to 37°C, adding prewarmed medium containing drug. After the indicated time points, the cells were chilled on ice, followed by treatment with TCEP or reaction buffer in the cold. After quenching of residual TCEP with iodoacetamide, the cells were lysed, and the total viral GP2 was isolated via immunoprecipitation (IP) with MAb 83.6 as described previously (70). Immunocomplexes were separated by SDS-PAGE, and biotinylated GP2 was detected by Western blotting under nonreducing conditions using horseradish peroxidase (HRP)-conjugated streptavidin. In specimens treated with reaction buffer only, we observed similar virus binding to A549 cells in the presence or absence of TRAM-34, excluding blocking of receptor binding by the drug (Fig. 6B). In cells treated with TCEP, the kinetics of virus internalization was unaffected by the drug (Fig. 6B), indicating that TRAM-34 does not interfere with endocytosis.

Since the data suggested that TRAM-34 targets a later viral entry step, we assessed a possible effect of the drug on arenavirus fusion using a quantitative split luciferase-based fusion assay, schematically shown in Fig. 7A. In this assay format, LCMV and

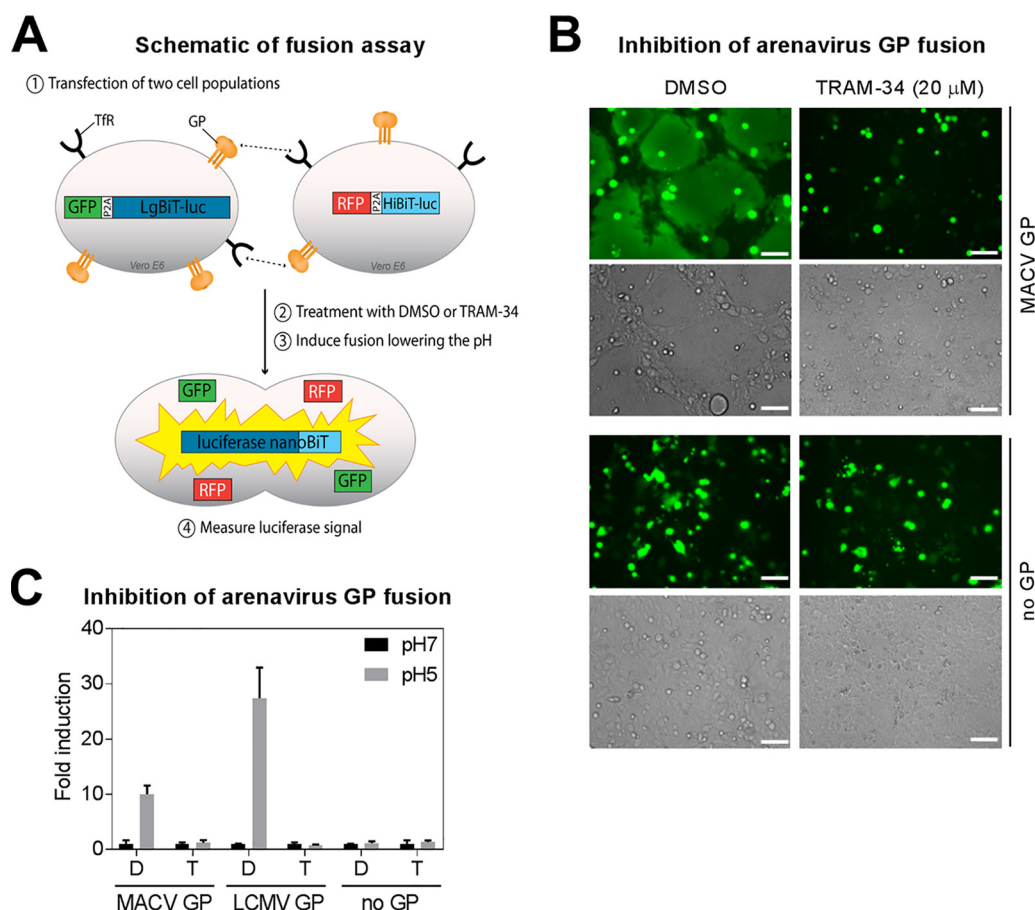


FIG 7 TRAM-34 inhibits low-pH-induced arenavirus GP fusion. (A) Schematic of the split nanoluciferase-based quantitative fusion assay based on NanoLuc Binary Technology (NanoBiT). Different cell populations were transfected with MACV or LCMV clone-13 GPC, together with pRRL-RFP-P2A-HiBiT or MACV or LCMV clone-13 GPC in combination with pRRL-GFP-P2A-LgBiT. After coculture for 24 h, the cells were treated with 20 μ M TRAM-34 or DMSO control, and fusion was induced at the cell surface by lowering the medium pH (5.0) in the presence of drugs for 20 min. Acidified medium was removed, and fresh medium was added, followed by incubation for 16 h at 37°C. The nanoluciferase signal was detected by Nano-Glo live cell assay. (B) Example of a split nanoluciferase fusion assay in presence or absence of transfected GP and treatment with 20 μ M TRAM-34 or DMSO. Please note that syncytium formation occurred only in the presence of expressed GP and in the absence of TRAM-34. Scale bar, 100 μ m. (C) TRAM-34 inhibits membrane fusion mediated by recombinant MACV and LCMV GP. Cells were cotransfected with the indicated arenavirus GP and the NanoBiT plasmids as in panel A. Low pH fusion was induced in the presence of 20 μ M TRAM-34 (T) or DMSO control (D) and the luciferase activity quantified by Nano-Glo Live Cell assay. The results are RLU normalized to the control (pH 7) and are means \pm the SD ($n = 3$).

MACV GPC were cotransfected into cells expressing either of the two halves of a split nanoluciferase reporter (LgBiT and HiBiT; NanoBiT technology, Promega). Both fragments were expressed in combination with GFP or red fluorescent protein (RFP), respectively, by using a “P2A” approach, which is based on a “self-cleaving” small peptide originally discovered in picornaviruses. After successful transfection, verified by detection of GFP and RFP in live cells, the two cell populations were cocultured, resulting in a mosaic of GP/LgBiT/GFP and GP/HiBiT/RFP cells. Arenavirus GP-mediated fusion was induced at the cell surface by treatment with low-pH buffer (pH 5.0) mimicking late endosomal conditions, as described previously (71). Exposure of arenavirus GP-transfected cells to low pH triggered extensive syncytium formation that was abolished by the presence of TRAM-34 (Fig. 7B). Quantification of fusion using the split nanoluciferase reporter revealed specific inhibition of cell-cell fusion mediated by MACV GP and LCMV GP by TRAM-34 (Fig. 7C). In sum, the data indicate that TRAM-34 specifically inhibits arenavirus fusion, revealing a novel and unexpected mechanism of antiviral action of clotrimazole drugs.

DISCUSSION

Over the past years, broad-spectrum antiviral agents such as ribavirin (5, 72) and favipiravir (73, 74) were successfully evaluated against major human-pathogenic arenaviruses and ribavirin is currently used in the clinic to treat human Lassa fever. However, considering the virulence and high mutation rates of human-pathogenic emerging arenaviruses, monotherapy has its limitations. Cocktails of antiviral drugs that target different steps of the viral life cycle appear as a promising strategy to limit viral multiplication and lower the risk of emergence of drug resistance. Targeting viral entry of highly pathogenic arenaviruses allows blocking the pathogen before it can take control of the host cell and blunt innate and adaptive antiviral defenses. The advent of arenavirus reverse genetics and recombinant pseudotype platforms allowed successful screening of small molecule libraries for entry inhibitors. These screens identified a panel of potent direct antiviral agents that target predominantly viral entry and show distinct specificities among arenaviruses (71, 75–81). A complementary approach involves the identification of cellular factors required for productive viral entry and their evaluation as antiviral drug targets. Among these candidate cellular factors, kinases, proteases, and ion channels that are already under evaluation as drug targets for the therapeutic intervention in other human disease are of particular interest, allowing repurposing existing drugs or drug candidates for antiviral therapy. This is illustrated by the recent identification of VGCC antagonists as novel entry inhibitors for JUNV (33). To this end, we employed an optimized VSV pseudotype platform that allowed rapid generation of a panel of VSV pseudotypes at robust titers, including some emerging viruses, whose envelope glycoproteins (GPs) are more difficult to incorporate (82, 83). Using this pseudotype platform, we identified the clotrimazole derivative TRAM-34, a specific inhibitor of the KCa3.1 channel, as a novel specific arenavirus entry inhibitor.

The synthetic triarylmethane clotrimazole was discovered in the 1970s as an inhibitor of fungal cell wall biosynthesis and originally proposed as a broad-spectrum antifungal drug (84). A remarkable specificity of clotrimazole for KCa3.1 was observed in patch-clamp studies after the discovery of the channel in 1997 (85). However, its relatively high toxicity due to cytochrome P450 inhibition limited its clinical use (86). Considering the potential of KCa3.1 as a drug target (34), clotrimazole analogues lacking P450-based toxicity were developed, including TRAM-34 and senicapoc. These drugs combine high potency with a remarkable selectivity (>200-fold) that is unusual among channel-blocking compounds (34). Their exquisite selectivity prevents perturbation of other voltage-gated potassium, calcium, sodium, and chloride channels, as well as ligand-gated ion channels, and therefore limits unwanted off-target side effects. Mice deficient in KCa3.1 show normal overall physiology, reproduction rate, and immune functions, indicating that even complete blocking of the channel does not affect viability (87). Moreover, TRAM-34 and senicapoc show favorable pharmacokinetics, long *in vivo* half-life, and are tolerated well (34, 88). Over the past decade, TRAM-34 and senicapoc have been evaluated in experimental *in vitro* and *in vivo* studies against a range of important human diseases, including sickle cell anemia (39), vascular disease (40), obliterative airway disease (41), malaria (42), and stroke (45).

To investigate the specific role of KCa3.1 in the observed antiviral effect of clotrimazoles, we first compared the antiviral activity of clotrimazole, TRAM-34, and senicapoc with the structurally unrelated selective KCa3.1 inhibitor NS6180 (66). Similar to the recent evaluation of clotrimazoles as candidate antimalaria drugs (42), we found no direct correlation between antiviral potency and on-target efficacy. Deletion of KCa3.1 from susceptible human cells by CRISPR/Cas9 had no effect on the antiviral activity of clotrimazoles. In sum, this indicated a yet unknown antiviral effect of clotrimazole derivatives that was apparently independent of the known mechanism-based drug action, but possibly linked to their unique triarylmethane structure.

Using a specific assay that allows monitoring of early viral entry steps, we were able to exclude antiviral activity of TRAM-34 at the level of receptor binding and/or endocytosis. This fits with the distinct receptors specificities and endocytotic pathways used

by the different arenaviruses (18, 20, 21, 52, 53, 58, 89). Despite marked differences in receptor use and endocytosis, all currently known arenaviruses are delivered to acidified endosomes, where they undergo low-pH-induced membrane fusion at pH <5.5, characteristic for late penetrating viruses (90). In contrast to most arenaviruses, entry of the late-fusing LASV was unaffected, arguing against a general perturbation of late endosomal compartments. The resistance of LASV to clotrimazoles was not linked to its capacity to hijack LAMP-1 as late endosomal entry factor. Interestingly, the distantly related LUJV that hijacks CD63 as a late endosomal entry factor (20) remained sensitive to TRAM-34, albeit to a lesser degree. To assess a possible effect of TRAM-34 on arenavirus GP-mediated fusion in the absence of endocytosis, we used a well-established quantitative split luciferase-based cell-cell fusion assay. We observed specific inhibition of low-pH-induced fusion of both MACV GP and LCMV GP, pinpointing arenavirus fusion inhibitors as the actual drug target.

Recent structural studies on the prefusion conformation of arenaviruses revealed important differences in the architecture of the membrane-proximal fusion machinery of arenavirus GP2 compared to other class I viral fusion proteins (13, 14). These structural differences are linked to the particular composition of the mature fusion-competent SSP/GP1/GP2 trimer and the unusual mechanism of arenavirus fusion (29). The arenavirus SSP contains two distinct hydrophobic domains (91, 92), with both N and C termini located in the cytosol and associates noncovalently with the cytoplasmic domain of GP2 via a zinc-binding domain (93–96). This unique SSP/GP2 interface is crucial for pH sensing required for arenavirus fusion (97, 98) and represents a preferred target for several small molecule arenavirus fusion inhibitors (99–101).

The recent evaluation of a candidate small molecule arenavirus fusion inhibitor in a guinea pig model demonstrated significant protection, providing proof-of-concept (102). However, the relatively low *in vivo* stability of many candidate fusion inhibitors remains currently a limiting factor. To the best of our knowledge, they have so far not been evaluated in a nonhuman primate challenge model that represents the current gold standard. In our hands, TRAM-34 blocked arenavirus entry with an IC_{50} of 5 to 20 μ M for most arenaviruses. This micromolar IC_{50} is similar to the potency of ribavirin (103) and favipiravir (73), the currently most promising antiarenaviral drugs. Considering its favorable toxicity profile and high *in vivo* stability, this makes TRAM-34 at this point a useful experimental drug. However, there is clearly room for improvement and enhanced potency will be needed prior to evaluation in nonhuman primate models. Previous structure-activity relationship (SAR) studies aiming at improved on-target efficacy resulted in collections of clotrimazole derivatives (42). Since the antiviral effect seems independent of the pharmacological drug target, the SAR profiles against the viral GP may be different. Our arenavirus pseudotype platform opens the possibility to rescreen existing collections of small molecule compounds against a panel of arenaviruses to identify more potent candidate compounds. The large body of existing data on the toxicity, pharmacokinetics and pharmacodynamics for clotrimazole derivatives may facilitate repurposing these established drugs, shortcutting some of the time-consuming and cost-intensive steps of human drug development. With this, clotrimazole derivatives may help to combat human arenavirus infection in postexposure prophylaxis and in therapy, combined with already established inhibitors of viral replication like favipiravir and ribavirin.

MATERIALS AND METHODS

Antibodies and reagents. MAb to TCRV NP has been described (104), as have been MAb 113 anti-LCMV NP (105), MAb 83.6 to LCMV GP2 (106), and MAb I-1 to VSV G (48). Mouse MAb sc-20011 anti-LAMP-1 was from Santa Cruz Biotechnology. Mouse MAb B-5-1-2 anti- α -tubulin was from Sigma-Aldrich. HRP-conjugated polyclonal goat anti-mouse IgG was from Dako. Fluorescein isothiocyanate-conjugated goat anti-mouse IgG was from Jackson Immuno Research. The nuclear dye DAPI (4',6'-diamidino-2-phenylindole) was purchased from Molecular Probes (Eugene, OR). Clotrimazole and senicapoc were obtained from MedChem Express, TRAM-34 was obtained from Sigma, and NS6180 was obtained from Alomone. Ammonium chloride (NH_4Cl) and EIPA were purchased from Sigma. The inhibitor PF-429242 has been described previously (107). NucBlue Live ReadyProbes reagent was

performed by limiting dilution in 96-well tissue culture plates. Due to lack of appropriate antibodies, TA cloning in combination with sequencing was used to validate KCNN4 knock out cells. A TA cloning kit (Life Technologies, K202020) was used according to the manufacturer's instructions to sequence DNA fragment containing the region where Cas9 was guided by a sgRNA.

(ii) Generation of LAMP-1-deficient A549 cells. Two guide RNAs (gRNAs) targeting the second exon of LAMP-1 were selected using the CRISPR design tool (<http://crispr.mit.edu/>). Primers for both strands covering the two cleavage sites (1F, 5'-**CAC CGC** TGC TGA CGC ACA ATG CAT G-3'; 1R, 5'-**AAA CCA** TGC ATT GTG CGT CAG CAG **C-3'**; 2F, 5'-**CAC CGC** AAC GGG ACC GCG TGC ATA A-3'; 2R, 5'-**AAA CTT** ATG CAC GCG GTC CCG TTG **C-3'** [boldfaced letters indicate the complementary Esp3I overhangs]) were annealed to generate a double-stranded oligonucleotide that was cloned into the Esp3I site of a lentiCRISPR v2 (Addgene, catalog no. 52961). Correct insertion of the two gRNA was confirmed by sequencing. Each gRNA cloned into the lentiCRISPR v2 vector was cotransfected with psPAX2 (a vector encoding Gag and Pol from HIV) and pMD2.G (a VSV-G-expressing envelope plasmid) into HEK 293T cells using Lipofectamine 3000 (Thermo Fisher), in order to generate lentivirus. At 48 h after transfection, lentiviruses carrying gRNA1 and gRNA2 were collected separately and used to simultaneously infect A549 cells for genome editing. At 48 h after infection, 1.5 μ g/ml of puromycin (Sigma-Aldrich) was added to select infected cells, and the samples were kept for 5 days. The resistant population was subsequently amplified and checked for LAMP-1 knockout by Western blotting. To obtain single-cell-derived clones, LAMP-1-deficient A549 were plated at 1 cell/ml in a 96-well plate in 250 μ l and then grown for 1 month, refreshing the medium twice a week. Seven clones were selected and amplified, and LAMP-1 deficiency was verified by Western blotting.

Immunoblotting. For immunoblotting, proteins were separated by SDS-PAGE and transferred to nitrocellulose. After blocking in 5% (wt/vol) skim milk in PBS, membranes were incubated with 1 to 10 μ g/ml primary antibody in 5% (wt/vol) skim milk and PBS overnight at 4°C. After several washes in PBS–0.1% (wt/vol) Tween 20 (PBST), secondary antibodies coupled to HRP were applied 1: 5,000 in PBST for 1 h at room temperature. Membranes were developed by enhanced chemiluminescence (ECL) using a LiteABlot kit (EuroClone). Signals were acquired by ImageQuant LAS 4000Mini (GE Healthcare Life Sciences) or by exposure to X-ray films. Quantification of Western blots was performed with ImageQuant TL (GE Healthcare Life Sciences).

Virus internalization assay. LCMV clone-13 was produced in BHK-21 cells and purified over a renografin gradient as described previously (116). Purified virus was diluted in PBS and labeled with the thiol-cleavable reagent NHS-SS-biotin (Pierce) as reported (69). The cleavage of the biotin label was verified by reaction with the membrane-impermeable reducing agent Tris(2-carboxyethyl)phosphine (TCEP; 10 mM; Pierce) for 30 min, which resulted in a loss of >95% of the biotin label. An internalization assay was performed as described previously (67). Briefly, 4×10^5 A549 cells were seeded per well of 6-well tissue culture plates to obtain closed monolayers. Medium was removed, and cells washed twice with cold Hanks balanced salt solution (HBSS) and chilled on ice for 5 min. A cold solution containing NHS-SS-biotinylated LCMV (50 particles/cell) in HBSS was added. After incubation for 1 h on ice, unbound virus was removed, and the cells were washed with cold HBSS. For internalization, cells were rapidly shifted to 37°C by adding prewarmed complete medium. After the indicated incubation times, medium was removed and cells chilled on ice. TCEP (15 mM) in 50 mM HEPES (pH 7.5), 150 mM NaCl, 1 mM CaCl_2 , and 1 mM MgCl_2 was added (1 ml/well) and applied twice for 15 min on ice. Cells were washed three times with cold HBSS, and the remaining TCEP was quenched with 100 mM iodoacetamide in HBSS for 10 min, followed by cell lysis using 1% (wt/vol) Triton X-100, 0.1% (wt/vol) SDS, 50 mM Tris-HCl (pH 7.5), 150 mM NaCl, 1 mM EDTA, 1 mM phenylmethylsulfonyl fluoride, and protease cOmplete inhibitor (Roche). To cleared lysates, 10^7 PFU purified, unlabeled LCMV was added as carrier. LCMV GP2 was isolated by IP using MAb 83.6 anti-LCMV GP2 immobilized on Sepharose 4B as described previously (67). Immunocomplexes were separated by nonreducing SDS-PAGE. Biotinylated LCMV GP2 was detected by Western blotting with HRP-conjugated streptavidin using ECL for detection.

Split nanoluciferase-based quantitative fusion assay. The split nanoluciferase-based quantitative fusion assay is based on NanoLuc Binary Technology (NanoBiT) from Promega and the plasmids were optimized and engineered by adding GFP or RFP reporters. On the first day, VeroE6 cells were seeded at 30,000 cells/well in a Costar white clear bottom 96-well tissue culture plates and at 800,000 cells/well in a M6 plate. After 6 h, cells in 96-well tissue culture plates were transfected with MACV or LCMV clone-13 GPC, together with pRRL-RFP-P2A-HiBiT, and cells in 6-well tissue culture plates were transfected with MACV or LCMV clone-13 GPC, together with pRRL-GFP-P2A-LgBiT. We used Lipofectamine 3000 (Thermo Fisher) as a transfection reagent according to the manufacturer's instructions. On day 2, cells in 6-well tissue culture plate were detached using TrypLE Express (Gibco), and 40,000 cells were seeded on top of transfected Vero E6 cells cultured in a 96-well tissue culture plate, resulting in cocultures. After 24 h of incubation at 37°C and 5% CO_2 , cells were pretreated for 1 h with 20 μ M TRAM-34 or dimethyl sulfoxide (DMSO). In order to trigger fusion, cells were incubated for 20 min at 37°C and 5% CO_2 with a low-pH medium in the presence of 20 μ M TRAM-34 or DMSO. The low-pH medium was composed of DMEM GlutaMAX (Gibco), supplemented with 10% (vol/vol) FCS (Amimed), 10 mM HEPES, and 10 mM MES, with the pH adjusted to 5 using concentrated HCl. The acidic medium was removed and replaced with fresh DMEM GlutaMAX and 10% (vol/vol) FCS, and the cells were incubated overnight at 37°C and 5% CO_2 . On day 4, the nanoluciferase signal was measured by using the Nano-Glo live cell assay system according to the manufacturer's instructions.

ACKNOWLEDGMENTS

We thank Ron Diskin (Department of Structural Biology, Weizmann Institute of Science, Rehovot, Israel) for the expression plasmid for the LASV GP mutant H230E. We acknowledge Juan Carlos de la Torre (Scripps Research Institute, La Jolla, CA) for the expression vector for TCRV GPC, TCRV virus, rLCMV, and MAb I1 to VSV G. We thank Connie Schmaljohn (USAMRIID, Fort Detrick, MD) for the plasmid pWRG/HTNV-M encoding HTNV GPC and Nicole Tischler (Fundación Ciencia & Vida, Santiago, Chile) for the plasmid pl.18 encoding ANDV GPC.

This research was supported by Swiss National Science Foundation grants 310030_149746 and 310030_170108 to S.K. and funds to S.K. from the University of Lausanne. C.W. is supported by grants from the Swiss National Science Foundation (CRSII3_154420, 31003A_160181/1, and IZCSZ0-174639). Funding was provided by the Swiss Food Safety and Veterinary Office (project 1.13.09) to G.Z. and Swiss National Science Foundation grant 310030_173185 to P.P. Further support was provided by the Swiss Federal Office for Civil Protection (grant 353006233/Stm to O.E. and S.K.).

REFERENCES

- Bonthius DJ. 2009. Lymphocytic choriomeningitis virus: a prenatal and postnatal threat. *Adv Pediatr* 56:75–86. <https://doi.org/10.1016/j.yapd.2009.08.007>.
- Palacios G, Druce J, Du L, Tran T, Birch C, Briese T, Conlan S, Quan PL, Hui J, Marshall J, Simons JF, Egholm M, Paddock CD, Shieh WJ, Goldsmith CS, Zaki SR, Catton M, Lipkin WI. 2008. A new arenavirus in a cluster of fatal transplant-associated diseases. *N Engl J Med* 358:991–998. <https://doi.org/10.1056/NEJMoa073785>.
- McCormick JB, Fisher-Hoch SP. 2002. Lassa fever. *Curr Top Microbiol Immunol* 262:75–109.
- Briese T, Paweska JT, McMullan LK, Hutchison SK, Street C, Palacios G, Khristova ML, Weyer J, Swanepoel R, Egholm M, Nichol ST, Lipkin WI. 2009. Genetic detection and characterization of Lujo virus, a new hemorrhagic fever-associated arenavirus from southern Africa. *PLoS Pathog* 5:e1000455. <https://doi.org/10.1371/journal.ppat.1000455>.
- Sarute N, Ross SR. 2017. New World arenavirus biology. *Annu Rev Virol* 4:141–158. <https://doi.org/10.1146/annurev-virology-101416-042001>.
- Andersen KG, Shapiro BJ, Matranga CB, Sealfon R, Lin AE, Moses LM, Folarin OA, Goba A, Odia I, Ehiane PE, Momoh M, England EM, Winnicki S, Branco LM, Gire SK, Phelan E, Tariyal R, Tewhey R, Omoniwa O, Fullah M, Fonnier R, Fonnier M, Kanneh L, Jalloh S, Gbakie M, Saffa S, Karbo K, Gladden AD, Qu J, Stremlau M, Nekoui M, Finucane HK, Tabrizi S, Vittori JJ, Birren B, Fitzgerald M, McCowan C, Ireland A, Berlin AM, Boichicchio J, Tazon-Vega B, Lennon NJ, Ryan EM, Bjornson Z, Milner DA, Lukens AK, Broddie N, Rowland M, Heinrich M, Akdag M, Schieffelin JS, Levy D, Akpan H, Bausch DG, Rubins K, McCormick JB, Lander ES, Günther S, Hensley L, Okogbenin S, Schaffner SF, Okokhere PO, Khan SH, Grant DS, Akpede GO, Asogun DA, Gniurke A, Levin JZ, Happi CT, Garry RF, Sabeti PC. 2015. Clinical sequencing uncovers origins and evolution of Lassa virus. *Cell* 162:738–750. <https://doi.org/10.1016/j.cell.2015.07.020>.
- Geisbert TW, Jahrling PB. 2004. Exotic emerging viral diseases: progress and challenges. *Nat Med* 10:S110–S121. <https://doi.org/10.1038/nm1142>.
- Yun NE, Walker DH. 2012. Pathogenesis of Lassa fever. *Viruses* 4:2031–2048. <https://doi.org/10.3390/v4102031>.
- Stephenson EH, Larson EW, Dominik JW. 1984. Effect of environmental factors on aerosol-induced Lassa virus infection. *J Med Virol* 14:295–303.
- Borio L, Inglesby T, Peters CJ, Schmaljohn AL, Hughes JM, Jahrling PB, Ksiazek T, Johnson KM, Meyerhoff A, O'Toole T, Ascher MS, Bartlett J, Breman JG, Eitzen EM, Jr, Hamburg M, Hauer J, Henderson DA, Johnson RT, Kwik G, Layton M, Lillibridge S, Nabel GJ, Osterholm MT, Perl TM, Russell P, Tonat K. 2002. Hemorrhagic fever viruses as biological weapons: medical and public health management. *JAMA* 287:2391–2405.
- Buchmeier MJ, de la Torre JC, Peters CJ. 2007. *Arenaviridae*: the viruses and their replication, p 1791–1828. In Knipe DL, Howley PM (ed), *Fields virology*, 4th ed. Lippincott-Raven, Philadelphia, PA.
- Burri DJ, da Palma JR, Kunz S, Pasquato A. 2012. Envelope glycoprotein of arenaviruses. *Viruses* 4:2162–2181. <https://doi.org/10.3390/v4102162>.
- Hastie KM, Igonet S, Sullivan BM, Legrand P, Zandonatti MA, Robinson JE, Garry RF, Rey FA, Oldstone MB, Saphire EO. 2016. Crystal structure of the prefusion surface glycoprotein of the prototypic arenavirus LCMV. *Nat Struct Mol Biol* 23:513–521. <https://doi.org/10.1038/nsmb.3210>.
- Hastie KM, Zandonatti MA, Kleinfelter LM, Heinrich ML, Rowland MM, Chandran K, Branco LM, Robinson JE, Garry RF, Saphire EO. 2017. Structural basis for antibody-mediated neutralization of Lassa virus. *Science* 356:923–928. <https://doi.org/10.1126/science.aam7260>.
- Eschli B, Quirin K, Wepf A, Weber J, Zinkernagel R, Hengartner H. 2006. Identification of an N-terminal trimeric coiled-coil core within arenavirus glycoprotein 2 permits assignment to class I viral fusion proteins. *J Virol* 80:5897–5907. <https://doi.org/10.1128/JVI.00008-06>.
- Borrow P, Oldstone MB. 1992. Characterization of lymphocytic choriomeningitis virus-binding protein(s): a candidate cellular receptor for the virus. *J Virol* 66:7270–7281.
- Wright KE, Salvato MS, Buchmeier MJ. 1989. Neutralizing epitopes of lymphocytic choriomeningitis virus are conformational and require both glycosylation and disulfide bonds for expression. *Virology* 171:417–426.
- Cao W, Henry MD, Borrow P, Yamada H, Elder JH, Ravkov EV, Nichol ST, Compans RW, Campbell KP, Oldstone MB. 1998. Identification of alpha-dystroglycan as a receptor for lymphocytic choriomeningitis virus and Lassa fever virus [see comments]. *Science* 282:2079–2081.
- Spiropoulou CF, Kunz S, Rollin PE, Campbell KP, Oldstone MB. 2002. New World arenavirus clade C, but not clade A and B viruses, utilizes alpha-dystroglycan as its major receptor. *J Virol* 76:5140–5146. <https://doi.org/10.1128/JVI.76.10.5140-5146.2002>.
- Raaben M, Jae LT, Herbert AS, Kuehne AI, Stubbs SH, Chou YY, Blomen VA, Kirchhausen T, Dye JM, Brummelkamp TR, Whelan SP. 2017. NRP2 and CD63 are host factors for Lujo virus cell entry. *Cell Host Microbe* 22:688–696.e5. <https://doi.org/10.1016/j.chom.2017.10.002>.
- Radoshitzky SR, Abraham J, Spiropoulou CF, Kuhn JH, Nguyen D, Li W, Nagel J, Schmidt PJ, Nunberg JH, Andrews NC, Farzan M, Choe H. 2007. Transferrin receptor 1 is a cellular receptor for New World hemorrhagic fever arenaviruses. *Nature* 446:92–96. Epub 2007 Feb 7. <https://doi.org/10.1038/nature05539>.
- Radoshitzky SR, Kuhn JH, Spiropoulou CF, Albarino CG, Nguyen DP, Salazar-Bravo J, Dorfman T, Lee AS, Wang E, Ross SR, Choe H, Farzan M. 2008. Receptor determinants of zoonotic transmission of New World hemorrhagic fever arenaviruses. *Proc Natl Acad Sci U S A* 105:2664–2669. <https://doi.org/10.1073/pnas.0709254105>.
- Abraham J, Kwong JA, Albarino CG, Lu JG, Radoshitzky SR, Salazar-Bravo J, Farzan M, Spiropoulou CF, Choe H. 2009. Host-species transferrin receptor 1 orthologs are cellular receptors for nonpathogenic new world clade B arenaviruses. *PLoS Pathog* 5:e1000358. <https://doi.org/10.1371/journal.ppat.1000358>.
- Fedeli C, Torriani G, Galan-Navarro C, Moraz ML, Moreno H, Gerold G, Kunz S. 2018. Axl can serve as entry factor for Lassa virus depending on

- the functional glycosylation of dystroglycan. *J Virol* 92:e01613-17. <https://doi.org/10.1128/JVI.01613-17>.
25. Brouillette RB, Phillips EK, Patel R, Mahaud-Fernandez W, Moller-Tank S, Rogers KJ, Dillard JA, Cooney AL, Martinez-Sobrido L, Okeoma C, Maury W. 2018. TIM-1 mediates dystroglycan-independent entry of Lassa virus. *J Virol* <https://doi.org/10.1128/JVI.00093-18>.
26. Shimajima M, Stroher U, Ebihara H, Feldmann H, Kawaoka Y. 2012. Identification of cell surface molecules involved in dystroglycan-independent Lassa virus cell entry. *J Virol* 86:2067–2078. <https://doi.org/10.1128/JVI.06451-11>.
27. Jemielity S, Wang JJ, Chan YK, Ahmed AA, Li W, Monahan S, Bu X, Farzan M, Freeman GJ, Umetsu DT, Dekruyff RH, Choe H. 2013. TIM-family proteins promote infection of multiple enveloped viruses through virion-associated phosphatidylserine. *PLoS Pathog* 9:e1003232. <https://doi.org/10.1371/journal.ppat.1003232>.
28. Pasqual G, Rojek JM, Masin M, Chatton JY, Kunz S. 2011. Old World arenaviruses enter the host cell via the multivesicular body and depend on the endosomal sorting complex required for transport. *PLoS Pathog* 7:e1002232. <https://doi.org/10.1371/journal.ppat.1002232>.
29. Nunberg JH, York J. 2012. The curious case of arenavirus entry, and its inhibition. *Viruses* 4:83–101. <https://doi.org/10.3390/v4010083>.
30. Igonet S, Vaney M-C, Vonrhein C, Vohrheine C, Bricogne G, Stura EA, Hengartner H, Eschli B, Rey FA. 2011. X-ray structure of the arenavirus glycoprotein GP2 in its postfusion hairpin conformation. *Proc Natl Acad Sci U S A* 108:19967–19972. <https://doi.org/10.1073/pnas.1108910108>.
31. Parsy ML, Harlos K, Huiskonen JT, Bowden TA. 2013. Crystal structure of Venezuelan hemorrhagic fever virus fusion glycoprotein reveals a class 1 postfusion architecture with extensive glycosylation. *J Virol* 87:13070–13075. <https://doi.org/10.1128/JVI.02298-13>.
32. Jae LT, Raaben M, Herbert AS, Kuehne AI, Wirchnianski AS, Soh TK, Stubbs SH, Janssen H, Damme M, Saftig P, Whelan SP, Dye JM, Brummelkamp TR. 2014. Virus entry: Lassa virus entry requires a trigger-induced receptor switch. *Science* 344:1506–1510. <https://doi.org/10.1126/science.1252480>.
33. Lavanya M, Cuevas CD, Thomas M, Cherry S, Ross SR. 2013. siRNA screen for genes that affect Junin virus entry uncovers voltage-gated calcium channels as a therapeutic target. *Sci Transl Med* 5:204ra131. <https://doi.org/10.1126/scitranslmed.3006827>.
34. Chou CC, Lunn CA, Murgolo NJ. 2008. KCa3.1: target and marker for cancer, autoimmune disorder and vascular inflammation? *Expert Rev Mol Diagn* 8:179–187. <https://doi.org/10.1586/14737159.8.2.179>.
35. Albaum M, Srivastava S, Li Z, Zhdnova O, Wulff H, Itani O, Wallace DP, Skolnik EY. 2008. KCa3.1 potassium channels are critical for cAMP-dependent chloride secretion and cyst growth in autosomal-dominant polycystic kidney disease. *Kidney Int* 74:740–749. <https://doi.org/10.1038/ki.2008.246>.
36. Klein H, Garneau L, Trinh NT, Prive A, Dionne F, Goupil E, Thuringer D, Parent L, Brochiero E, Sauve R. 2009. Inhibition of the KCa3.1 channels by AMP-activated protein kinase in human airway epithelial cells. *Am J Physiol Cell Physiol* 296:C285–C295. <https://doi.org/10.1152/ajpcell.00418.2008>.
37. Harron SA, Clarke CM, Jones CL, Babin-Muise D, Cowley EA. 2009. Volume regulation in the human airway epithelial cell line Calu-3. *Can J Physiol Pharmacol* 87:337–346. <https://doi.org/10.1139/y09-009>.
38. Arthur GK, Duffy SM, Roach KM, Hirst RA, Shikotra A, Gaillard EA, Bradding P. 2015. KCa3.1 K⁺ channel expression and function in human bronchial epithelial cells. *PLoS One* 10:e0145259. <https://doi.org/10.1371/journal.pone.0145259>.
39. Ataga KI, Smith WR, De Castro LM, Swerdlow P, Sauntharajah Y, Castro O, Vichinsky E, Kutlar A, Orringer EP, Rigdon GC, Stocker JW, Investigators ICA. 2008. Efficacy and safety of the Gardos channel blocker, senicapoc (ICA-17043), in patients with sickle cell anemia. *Blood* 111:3991–3997. <https://doi.org/10.1182/blood-2007-08-110098>.
40. Tharp DL, Bowles DK. 2009. The intermediate-conductance Ca²⁺-activated K⁺ channel (KCa3.1) in vascular disease. *Cardiovasc Hematol Agents Med Chem* 7:1–11.
41. Hua X, Deuse T, Chen YJ, Wulff H, Stubbendorff M, Kohler R, Miura H, Langer F, Reichenspurner H, Robbins RC, Schrepfer S. 2013. The potassium channel KCa3.1 as new therapeutic target for the prevention of obliterative airway disease. *Transplantation* 95:285–292. <https://doi.org/10.1097/TP.0b013e318275a2f4>.
42. Tubman VN, Mejia P, Shmukler BE, Bei AK, Alper SL, Mitchell JR, Brugnara C, Duraisingham MT. 2016. The clinically tested Gardos channel inhibitor senicapoc exhibits antimalarial activity. *Antimicrob Agents Chemother* 60:613–616. <https://doi.org/10.1128/AAC.01668-15>.
43. Wulff H, Miller MJ, Hanel W, Grissmer S, Cahalan MD, Chandy KG. 2000. Design of a potent and selective inhibitor of the intermediate-conductance Ca²⁺-activated K⁺ channel, IKCa1: a potential immunosuppressant. *Proc Natl Acad Sci U S A* 97:8151–8156.
44. Stocker JW, De Franceschi L, McNaughton-Smith GA, Corrocher R, Beuzard Y, Brugnara C. 2003. ICA-17043, a novel Gardos channel blocker, prevents sickled red blood cell dehydration *in vitro* and *in vivo* in SAD mice. *Blood* 101:2412–2418. <https://doi.org/10.1182/blood-2002-05-1433>.
45. Staal RGW, Weinstein JR, Nattini M, Cajina M, Chandresana G, Moller T. 2017. Senicapoc: repurposing a drug to target microglia KCa3.1 in stroke. *Neurochem Res* 42:2639–2645. <https://doi.org/10.1007/s11064-017-2223-y>.
46. Zimmer G, Locher S, Berger Rentsch M, Halbherr SJ. 2014. Pseudotyping of vesicular stomatitis virus with the envelope glycoproteins of highly pathogenic avian influenza viruses. *J Gen Virol* 95:1634–1639. <https://doi.org/10.1099/vir.0.065201-0>.
47. Moeschler S, Locher S, Zimmer G. 2018. 1-Benzyl-3-cetyl-2-methylimidazolium iodide (NH125) is a broad-spectrum inhibitor of virus entry with lysosomotropic features. *Viruses* 10:306. <https://doi.org/10.3390/v10060306>.
48. Holland JJ, de la Torre JC, Steinhauer DA, Clarke D, Duarte E, Domingo E. 1989. Virus mutation frequencies can be greatly underestimated by monoclonal antibody neutralization of virions. *J Virol* 63:5030–5036.
49. Pasquato A, Fernandez AH, Kunz S. 2018. Studies of Lassa virus cell entry. *Methods Mol Biol* 1604:135–155. https://doi.org/10.1007/978-1-4939-6981-4_9.
50. Ohkuma S, Poole B. 1978. Fluorescence probe measurement of the intralysosomal pH in living cells and the perturbation of pH by various agents. *Proc Natl Acad Sci U S A* 75:3327–3331.
51. Ohkuma S, Poole B. 1981. Cytoplasmic vacuolation of mouse peritoneal macrophages and the uptake into lysosomes of weakly basic substances. *J Cell Biol* 90:656–664.
52. Martinez MG, Cordo SM, Candurra NA. 2007. Characterization of Junin arenavirus cell entry. *J Gen Virol* 88:1776–1784. <https://doi.org/10.1099/vir.0.82808-0>.
53. Rojek JM, Sanchez AB, Nguyen NT, de la Torre JC, Kunz S. 2008. Different mechanisms of cell entry by human-pathogenic Old World and New World arenaviruses. *J Virol* 82:7677–7687. <https://doi.org/10.1128/JVI.00560-08>.
54. Lee AM, Cruite J, Welch MJ, Sullivan B, Oldstone MB. 2013. Pathogenesis of Lassa fever virus infection. I. Susceptibility of mice to recombinant Lassa Gp/LCMV chimeric virus. *Virology* <https://doi.org/10.1016/j.virol.2013.04.010>.
55. Goncalves AR, Moraz ML, Pasquato A, Helenius A, Lozach PY, Kunz S. 2013. Role of DC-SIGN in Lassa virus entry into human dendritic cells. *J Virol* 87:11504–11515. <https://doi.org/10.1128/JVI.01893-13>.
56. Mercer J, Helenius A. 2009. Virus entry by macropinocytosis. *Nat Cell Biol* 11:510–520. <https://doi.org/10.1038/ncb0509-510>.
57. Mercer J, Helenius A. 2012. Gulping rather than sipping: macropinocytosis as a way of virus entry. *Curr Opin Microbiol* 15:490–499. <https://doi.org/10.1016/j.mib.2012.05.016>.
58. Iwasaki M, Ngo N, de la Torre JC. 2014. Sodium hydrogen exchangers contribute to arenavirus cell entry. *J Virol* 88:643–654. <https://doi.org/10.1128/JVI.02110-13>.
59. Urata S, Yun N, Pasquato A, Paessler S, Kunz S, de la Torre JC. 2011. Antiviral activity of a small-molecule inhibitor of arenavirus glycoprotein processing by the cellular site 1 protease. *J Virol* 85:795–803. <https://doi.org/10.1128/JVI.02019-10>.
60. Pasquato A, Rochat C, Burri DJ, Pasqual G, de la Torre JC, Kunz S. 2012. Evaluation of the anti-arenaviral activity of the subtilisin kexin isozyme-1/site-1 protease inhibitor PF-429242. *Virology* 423:14–22. <https://doi.org/10.1016/j.virol.2011.11.008>.
61. Cohen-Dvashi H, Cohen N, Israeli H, Diskin R. 2015. Molecular mechanism for LAMP1 recognition by Lassa virus. *J Virol* 89:7584–7592. <https://doi.org/10.1128/JVI.00651-15>.
62. Li S, Sun Z, Pryce R, Parsy ML, Fehling SK, Schlie K, Siebert CA, Garten W, Bowden TA, Strecker T, Huiskonen JT. 2016. Acidic pH-Induced conformations and LAMP1 binding of the Lassa virus glycoprotein spike. *PLoS Pathog* 12:e1005418. <https://doi.org/10.1371/journal.ppat.1005418>.
63. Cohen-Dvashi H, Israeli H, Shani O, Katz A, Diskin R. 2016. Role of

- LAMP1 binding and pH sensing by the spike complex of Lassa virus. *J Virol* 90:10329–10338. <https://doi.org/10.1128/JVI.01624-16>.
64. Hulseberg CE, Feneant L, Szymanska KM, White JM. 2018. Lamp1 increases the efficiency of Lassa virus infection by promoting fusion in less acidic endosomal compartments. *mBio* 9:e01818-17. <https://doi.org/10.1128/mBio.01818-17>.
 65. Israeli H, Cohen-Dvashi H, Shulman A, Shimon A, Diskin R. 2017. Mapping of the Lassa virus LAMP1 binding site reveals unique determinants not shared by other old world arenaviruses. *PLoS Pathog* 13:e1006337. <https://doi.org/10.1371/journal.ppat.1006337>.
 66. Strobaek D, Brown DT, Jenkins DP, Chen YJ, Coleman N, Ando Y, Chiu P, Jorgensen S, Demnitz J, Wulff H, Christophersen P. 2013. NS6180, a new K(Ca) 3.1 channel inhibitor prevents T-cell activation and inflammation in a rat model of inflammatory bowel disease. *Br J Pharmacol* 168:432–444. <https://doi.org/10.1111/j.1476-5381.2012.02143.x>.
 67. Rojek JM, Perez M, Kunz S. 2008. Cellular entry of lymphocytic choriomeningitis virus. *J Virol* 82:1505–1517. <https://doi.org/10.1128/JVI.01331-07>.
 68. Pelkmans L, Puntener D, Helenius A. 2002. Local actin polymerization and dynamin recruitment in SV40-induced internalization of caveolae. *Science* 296:535–539. <https://doi.org/10.1126/science.1069784>.
 69. Moraz ML, Pythoud C, Turk R, Rothenberger S, Pasquato A, Campbell KP, Kunz S. 2013. Cell entry of Lassa virus induces tyrosine phosphorylation of dystroglycan. *Cell Microbiol* 15:689–700. <https://doi.org/10.1111/cmi.12078>.
 70. Kunz S, Edelmann KH, de la Torre J-C, Gorney R, Oldstone MBA. 2003. Mechanisms for lymphocytic choriomeningitis virus glycoprotein cleavage, transport, and incorporation into virions. *Virology* 314:168–178. [https://doi.org/10.1016/S0042-6822\(03\)00421-5](https://doi.org/10.1016/S0042-6822(03)00421-5).
 71. Lee AM, Rojek JM, Spiropoulou CF, Gundersen AT, Jin W, Shaginan A, York J, Nunberg JH, Boger DL, Oldstone MB, Kunz S. 2008. Unique small molecule entry inhibitors of hemorrhagic fever arenaviruses. *J Biol Chem* 283:18734–18742. <https://doi.org/10.1074/jbc.M802089200>.
 72. Parker WB. 2005. Metabolism and antiviral activity of ribavirin. *Virus Res* 107:165–171. <https://doi.org/10.1016/j.virusres.2004.11.006>.
 73. Delang L, Abdelnabi R, Neyts J. 2018. Favipiravir as a potential countermeasure against neglected and emerging RNA viruses. *Antiviral Res* 153:85–94. <https://doi.org/10.1016/j.antiviral.2018.03.003>.
 74. Furuta Y, Komeno T, Nakamura T. 2017. Favipiravir (T-705), a broad spectrum inhibitor of viral RNA polymerase. *Proc Jpn Acad Ser B Phys Biol Sci* 93:449–463. <https://doi.org/10.2183/pjab.93.027>.
 75. Bolken TC, Laquerre S, Zhang Y, Bailey TR, Pevear DC, Kickner SS, Sperzel LE, Jones KF, Warren TK, Amanda Lund S, Kirkwood-Watts DL, King DS, Shurtleff AC, Guttieri MC, Deng Y, Bleam M, Hruby DE. 2006. Identification and characterization of potent small molecule inhibitor of hemorrhagic fever New World arenaviruses. *Antiviral Res* 69:86–97. <https://doi.org/10.1016/j.antiviral.2005.10.008>.
 76. Larson RA, Dai D, Hosack VT, Tan Y, Bolken TC, Hruby DE, Amberg SM. 2008. Identification of a broad-spectrum arenavirus entry inhibitor. *J Virol* 82:10768–10775. <https://doi.org/10.1128/JVI.00941-08>.
 77. Ngo N, Henthorn KS, Cisneros MI, Cubitt B, Iwasaki M, de la Torre JC, Lama J. 2015. Identification and mechanism of action of a novel small-molecule inhibitor of arenavirus multiplication. *J Virol* 89:10924–10933. <https://doi.org/10.1128/JVI.01587-15>.
 78. Rathbun JY, Droniou ME, Damoiseaux R, Haworth KG, Henley JE, Exline CM, Choe H, Cannon PM. 2015. Novel arenavirus entry inhibitors discovered by using a minigenome rescue system for high-throughput drug screening. *J Virol* 89:8428–8443. <https://doi.org/10.1128/JVI.00997-15>.
 79. Dai D, Burgeson JR, Gharaibeh DN, Moore AL, Larson RA, Cerruti NR, Amberg SM, Bolken TC, Hruby DE. 2013. Discovery and optimization of potent broad-spectrum arenavirus inhibitors derived from benzimidazole. *Bioorg Med Chem Lett* 23:744–749. <https://doi.org/10.1016/j.bmcl.2012.11.095>.
 80. Burgeson JR, Gharaibeh DN, Moore AL, Larson RA, Amberg SM, Bolken TC, Hruby DE, Dai D. 2013. Lead optimization of an acylhydrazide scaffold possessing antiviral activity against Lassa virus. *Bioorg Med Chem Lett* 23:5840–5843. <https://doi.org/10.1016/j.bmcl.2013.08.103>.
 81. Burgeson JR, Moore AL, Gharaibeh DN, Larson RA, Cerruti NR, Amberg SM, Hruby DE, Dai D. 2013. Discovery and optimization of potent broad-spectrum arenavirus inhibitors derived from benzimidazole and related heterocycles. *Bioorg Med Chem Lett* 23:750–756. <https://doi.org/10.1016/j.bmcl.2012.11.093>.
 82. Berger Rentsch M, Zimmer G. 2011. A vesicular stomatitis virus replicon-based bioassay for the rapid and sensitive determination of multi-species type I interferon. *PLoS One* 6:e25858. <https://doi.org/10.1371/journal.pone.0025858>.
 83. Moeschler S, Locher S, Conzelmann KK, Kramer B, Zimmer G. 2016. Quantification of lyssavirus-neutralizing antibodies using vesicular stomatitis virus pseudotype particles. *Viruses* 8:E254.
 84. Burgess MA, Bodey GP. 1972. Clotrimazole (Bay b 5097): *in vitro* and clinical pharmacological studies. *Antimicrob Agents Chemother* 2:423–426.
 85. Ishii TM, Silvia C, Hirschberg B, Bond CT, Adelman JP, Maylie J. 1997. A human intermediate conductance calcium-activated potassium channel. *Proc Natl Acad Sci U S A* 94:11651–11656.
 86. Alvarez J, Montero M, Garcia-Sancho J. 1992. High-affinity inhibition of Ca²⁺-dependent K⁺ channels by cytochrome P-450 inhibitors. *J Biol Chem* 267:11789–11793.
 87. Begenisich T, Nakamoto T, Ovitt CE, Nehrke K, Brugnara C, Alper SL, Melvin JE. 2004. Physiological roles of the intermediate conductance, Ca²⁺-activated potassium channel Kcnn4. *J Biol Chem* 279:47681–47687. <https://doi.org/10.1074/jbc.M409627200>.
 88. Ataga KI, Orringer EP, Styles L, Vichinsky EP, Swerdlow P, Davis GA, Desimone PA, Stocker JW. 2006. Dose-escalation study of ICA-17043 in patients with sickle cell disease. *Pharmacotherapy* 26:1557–1564. <https://doi.org/10.1592/phco.26.11.1557>.
 89. Oppliger J, Torriani G, Herrador A, Kunz S. 2016. Lassa virus cell entry via dystroglycan involves an unusual pathway of macropinocytosis. *J Virol* 90:6412–6429. <https://doi.org/10.1128/JVI.00257-16>.
 90. Lozach PY, Huotari J, Helenius A. 2011. Late-penetrating viruses. *Curr Opin Virol* 1:35–43. <https://doi.org/10.1016/j.coviro.2011.05.004>.
 91. Eichler R, Lenz O, Strecker T, Eickmann M, Klenk HD, Garten W. 2003. Identification of Lassa virus glycoprotein signal peptide as a trans-acting maturation factor. *EMBO Rep* 4:1084–1088. <https://doi.org/10.1038/sj.embor.embor7400002>.
 92. York J, Romanowski V, Lu M, Nunberg JH. 2004. The signal peptide of the Junin arenavirus envelope glycoprotein is myristoylated and forms an essential subunit of the mature G1-G2 complex. *J Virol* 78:10783–10792. <https://doi.org/10.1128/JVI.78.19.10783-10792.2004>.
 93. Agnihothram SS, York J, Nunberg JH. 2006. Role of the stable signal peptide and cytoplasmic domain of G2 in regulating intracellular transport of the Junin virus envelope glycoprotein complex. *J Virol* 80:5189–5198. <https://doi.org/10.1128/JVI.00208-06>.
 94. Agnihothram SS, York J, Trahey M, Nunberg JH. 2007. Bitopic membrane topology of the stable signal peptide in the tripartite Junin virus GP-C envelope glycoprotein complex. *J Virol* 81:4331–4337. <https://doi.org/10.1128/JVI.02779-06>.
 95. York J, Nunberg JH. 2007. Distinct requirements for signal peptidase processing and function in the stable signal peptide subunit of the Junin virus envelope glycoprotein. *Virology* 359:72–81. <https://doi.org/10.1016/j.virol.2006.08.048>.
 96. Briknarova K, Thomas CJ, York J, Nunberg JH. 2011. Structure of a zinc-binding domain in the Junin virus envelope glycoprotein. *J Biol Chem* 286:1528–1536. <https://doi.org/10.1074/jbc.M110.166025>.
 97. York J, Nunberg JH. 2009. Intersubunit interactions modulate pH-induced activation of membrane fusion by the Junin virus envelope glycoprotein GPC. *J Virol* 83:4121–4126. <https://doi.org/10.1128/JVI.02410-08>.
 98. York J, Nunberg JH. 2006. Role of the stable signal peptide of Junin arenavirus envelope glycoprotein in pH-dependent membrane fusion. *J Virol* 80:7775–7780. <https://doi.org/10.1128/JVI.00642-06>.
 99. York J, Dai D, Amberg SM, Nunberg JH. 2008. pH-induced activation of arenavirus membrane fusion is antagonized by small-molecule inhibitors. *J Virol* 82:10932–10939. <https://doi.org/10.1128/JVI.01140-08>.
 100. Shankar S, Whitby LR, Casquilho-Gray HE, York J, Boger DL, Nunberg JH. 2016. Small-molecule fusion inhibitors bind the pH-sensing stable signal peptide-GP2 subunit interface of the Lassa virus envelope glycoprotein. *J Virol* 90:6799–6807. <https://doi.org/10.1128/JVI.00597-16>.
 101. Thomas CJ, Casquilho-Gray HE, York J, DeCamp DL, Dai D, Petrilli EB, Boger DL, Slayden RA, Amberg SM, Sprang SR, Nunberg JH. 2011. A specific interaction of small molecule entry inhibitors with the envelope glycoprotein complex of the Junin hemorrhagic fever arenavirus. *J Biol Chem* 286:6192–6200. <https://doi.org/10.1074/jbc.M110.196428>.
 102. Cashman KA, Smith MA, Twenhafel NA, Larson RA, Jones KF, Allen RD, Dai D, Chinsangaram J, Bolken TC, Hruby DE, Amberg SM, Hensley LE, Guttieri MC. 2011. Evaluation of Lassa antiviral compound ST-193 in a

- guinea pig model. *Antiviral Res* 90:70–79. <https://doi.org/10.1016/j.antiviral.2011.02.012>.
103. McCormick JB, King IJ, Webb PA, Scribner CL, Craven RB, Johnson KM, Elliott LH, Belmont-Williams R. 1986. Lassa fever: effective therapy with ribavirin. *N Engl J Med* 314:20–26. <https://doi.org/10.1056/NEJM198601023140104>.
 104. Sanchez A, Pifat DY, Kenyon RH, Peters CJ, McCormick JB, Kiley MP. 1989. Junin virus monoclonal antibodies: characterization and cross-reactivity with other arenaviruses. *J Gen Virol* 70:1125–1132. <https://doi.org/10.1099/0022-1317-70-5-1125>.
 105. Buchmeier MJ, Lewicki HA, Tomori O, Oldstone MB. 1981. Monoclonal antibodies to lymphocytic choriomeningitis and Pichinde viruses: generation, characterization, and cross-reactivity with other arenaviruses. *Virology* 113:73–85.
 106. Weber EL, Buchmeier MJ. 1988. Fine mapping of a peptide sequence containing an antigenic site conserved among arenaviruses. *Virology* 164:30–38.
 107. Hay BA, Abrams B, Zumbun AY, Valentine JJ, Warren LC, Petras SF, Shelly LD, Xia A, Varghese AH, Hawkins JL, Van Camp JA, Robbins MD, Landschulz K, Harwood HJ, Jr. 2007. Aminopyrrolidineamide inhibitors of site-1 protease. *Bioorg Med Chem Lett* 17:4411–4414. <https://doi.org/10.1016/j.bmcl.2007.06.031>.
 108. Perez M, Craven RC, de la Torre JC. 2003. The small RING finger protein Z drives arenavirus budding: implications for antiviral strategies. *Proc Natl Acad Sci U S A* 100:12978–12983. <https://doi.org/10.1073/pnas.2133782100>.
 109. Kunz S, Rojek JM, Perez M, Spiropoulou CF, Oldstone MB. 2005. Characterization of the interaction of Lassa fever virus with its cellular receptor alpha-dystroglycan. *J Virol* 79:5979–5987. <https://doi.org/10.1128/JVI.79.10.5979-5987.2005>.
 110. Rojek JM, Spiropoulou CF, Kunz S. 2006. Characterization of the cellular receptors for the South American hemorrhagic fever viruses Junin, Guanarito, and Machupo. *Virology* 349:476–491. <https://doi.org/10.1016/j.virol.2006.02.033>.
 111. Hooper JW, Custer DM, Thompson E, Schmaljohn CS. 2001. DNA vaccination with the Hantaan virus M gene protects hamsters against three of four HFRS hantaviruses and elicits a high-titer neutralizing antibody response in rhesus monkeys. *J Virol* 75:8469–8477.
 112. Cifuentes-Munoz N, Darlix JL, Tischler ND. 2010. Development of a lentiviral vector system to study the role of the Andes virus glycoproteins. *Virus Res* 153:29–35. <https://doi.org/10.1016/j.virusres.2010.07.001>.
 113. Dutko FJ, Oldstone MB. 1983. Genomic and biological variation among commonly used lymphocytic choriomeningitis virus strains. *J Gen Virol* 64:1689–1698. <https://doi.org/10.1099/0022-1317-64-8-1689>.
 114. Wolff S, Groseth A, Meyer B, Jackson D, Strecker T, Kaufmann A, Becker S. 2016. The New World arenavirus Tacaribe virus induces caspase-dependent apoptosis in infected cells. *J Gen Virol* 97:855–866. <https://doi.org/10.1099/jgv.0.000403>.
 115. Sanchez AB, de la Torre JC. 2006. Rescue of the prototypic Arenavirus LCMV entirely from plasmid. *Virology* 350:370–380. <https://doi.org/10.1016/j.virol.2006.01.012>.
 116. Kunz S, Sevilla N, Rojek JM, Oldstone MB. 2004. Use of alternative receptors different than alpha-dystroglycan by selected isolates of lymphocytic choriomeningitis virus. *Virology* 325:432–445. <https://doi.org/10.1016/j.virol.2004.05.009>.
 117. Shalem O, Sanjana NE, Hartenian E, Shi X, Scott DA, Mikkelsen TS, Heckl D, Ebert BL, Root DE, Doench JG, Zhang F. 2014. Genome-scale CRISPR-Cas9 knockout screening in human cells. *Science* 343:84–87. <https://doi.org/10.1126/science.1247005>.
 118. Ran FA, Hsu PD, Wright J, Agarwala V, Scott DA, Zhang F. 2013. Genome engineering using the CRISPR-Cas9 system. *Nat Protoc* 8:2281–2308. <https://doi.org/10.1038/nprot.2013.143>.
 119. Annibaldi A, Dousse A, Martin S, Tazi J, Widmann C. 2011. Revisiting G3BP1 as a RasGAP binding protein: sensitization of tumor cells to chemotherapy by the RasGAP 317–326 sequence does not involve G3BP1. *PLoS One* 6:e29024. <https://doi.org/10.1371/journal.pone.0029024>.